2.5 RF System for the Storage Ring

2.5.1 Introduction

The RF system for the SLS storage ring has a double task: compensating for the beam energy losses due to synchrotron radiation and providing the accelerating voltage necessary to achieve the required momentum acceptance. Several alternative versions have been considered and compared [1,2]. The solution which was adopted for the starting phase is based on the use of conventional, already well-proven equipment that should be available and operational within relatively short times, compatible with the SLS schedule. It essentially consists of four normal conducting (nc) single-cell 500 MHz cavities of the ELETTRA type, each powered with a 180 kW CW klystron amplifier via a WR1800 waveguide line [3].
The cavities with their input couplers, their tuning and cooling systems as well as the phase and amplitude regulation loops will be supplied by Sincrotone Trieste, the klystrons by EEV Ltd, the klystron supplies and control systems by THOMCAST AG.
The use of superconducting (sc) cavities has been ruled out as a starting solution. However, combining "HOM free" sc cavities with the initial nc system is regarded as a possible future option for improving the beam lifetime in the storage ring when operating at very high brightness (see section 2.7). Either the energy acceptance could be increased using one 500 MHz sc cavity [4,5], or the bunches could be lengthened using one (possibly two) higher harmonic sc cavity(ies) [6,7]. Within both schemes, the sc cavities could be operated in an entirely idle mode (no external RF source). This possible further upgrading is also discussed.

2.5.2 Design parameters

The basic parameters of the storage ring [8] which affect the RF system are listed in the upper part of Table t252_a.
The selection of the RF frequency was mainly dictated by the availability of commercial RF power sources and other components. We chose 500 MHz, the mostly used frequency. Moreover, it is a good compromise as regard to the equipment size, the required RF voltage and power as well as the corresponding bunch length. These quantities are related to the storage ring parameters as follows:

$$eV_{RF} = q\,\Delta U = \Delta U / \sin\phi_s;$$
$$\varepsilon_{RF} = [F(q)\,\Delta U / (\pi\,\alpha\,h\,E)]^{1/2}, \text{ where } F(q) = 2\,[(q^2 - 1)^{1/2} - \arccos(1/q)];$$
$$\sigma_s = c\,\alpha\,\sigma_p / (2\,\pi\,f_s), \text{ where } f_s = f_{RF}\,[\alpha\,V_{RF}\cos\phi_s / (2\,\pi\,h\,E/e)]^{1/2};$$
$$P_b = I_b\,\Delta U/e.$$

The definition of the notations used above as well as numerical values for the SLS are given in Table t252_a. The total RF power requirement, P_{RF} is then determined by the number of RF cavities, n_c and their shunt impedance, R_s:

$$P_{RF} = P_b + P_d,$$
where $P_d = V_{RF}^2 / (2\,n_c\,R_s)$ is the cavity wall dissipation.

We assumed here that the system was matched (zero reflected power) at full beam current. This condition which minimizes the maximum power requirement is fulfilled only if:

- the reactive component of the beam current is canceled by properly detuning the cavity so that the beam-loaded cavity is "seen" as a pure resistance;
- this equivalent resistance is matched to the RF source impedance by a correct setting of the coupling factor.

The detuning, Δf_m and the coupling factor, β_m satisfying these two conditions are given by:

$$\Delta f_m = (f_{RF} / 2 Q_o) (P_b / P_d) \cot g \phi_s ,$$
$$\beta_m = 1 + (P_b / P_d) ,$$

where Q_o is the unloaded cavity quality factor.

2.5.3 RF cavities and associated equipment

2.5.3.1 RF cavities

Four nc single-cell cavities of the ELETTRA type will provide the required RF voltage and power. They will be manufactured from high purity (99.99 %), high conductivity (HC), oxygen-free (OF) seamless copper forging and equipped with 8 equatorial outlet ports: 3 large ones - for the input power coupler, the pumping system, the plunger tuner - and 5 smaller ones for vacuum and RF monitoring. The cavity shape is shown in Figure f253_a and its main performance data are listed in Table t253_a [9].
The parameter values in Table t253_b show that, using four such cavities, the RF system has the potential for achieving the SLS requirement with a cavity input power lower than 150 kW. Besides, would one of the four cavities be out of use, the operation at full beam current is still possible with an RF voltage of about 2 MV.
The cavities will be accommodated in pairs in two of the dispersion free, low β, 4 m long straight sections of the storage ring (SS2 and SS8), as shown in Figure f253_b.
Values of shunt impedance 20 - 30 % larger could be obtained with nose cone (re-entrant) cavities [10-14], leading to a total power savings of about 10 %. Nevertheless, we selected the "elliptical" shape which is less susceptible to multipactor, and makes easier the cooling and manufacturing. Due to the relatively high beam power, low RF voltage and the practical limitations for the input couplers, the interest of multicell or sc cavities is rather limited here. Moreover the use of single cell cavities minimizes the number of Higher Order Modes (HOM) that could drive coupled bunch instabilities (see section 2.5.7).

2.5.3.2 Input couplers

The input coupler must be capable to feed into the cavity a CW RF power of at least 150 kW (forward) and also to handle the full reflection. It will be similar to those operating in ELETTRA which are of the coaxial type, terminated by a coupling loop. The air to vacuum transition is ensured by a cylindrical ceramic window brazed inside the coaxial line. Although the operating power at ELETTRA does not exceed 65 kW, the same coupler has successfully been tested up to 330 kW at DESY [15] and therefore should be capable to fulfil the SLS requirement. The coupling coefficient shall be adjustable within a range of 1 to 3.5 in order to match different beam loading conditions.
The coupler will be mounted on one of the three large cavity equatorial ports and connected to the WR1800 waveguide line by means of a standard 6-1/8" waveguide-to-coaxial transition (see Figure f253_b).

2.5.3.3 Cooling systems

The cavities are cooled by means of water flowing through pipes, brazed into channels which are machined around the cavity outer surface and outlet ports, as shown in Figure f253_a. This cooling circuit must be able to remove up to 65 kW of power dissipation into the cavity wall. In addition, it shall be possible - thanks to the cooling system - to set the cavity temperature at any value within 60 ± 25 °C with a stability of ± 0.05 °C (for $0 \leq Vacc \leq 650$ kV). This is achieved by properly isolating the cavity and by re-circulating the cooling water through an appropriate heat exchanger water station (cooling rack) dedicated to each cavity. The cavity

temperature is measured by a thermocouple, compared to a reference value and the error signal used for regulation in the cooling rack. Controlling the cavity operating temperature within the above specified range shall prevent coupled bunch instabilities with a beam current up to 400 mA (see section 2.5.7).

2.5.3.4 Frequency tuning systems

As mentioned before, the HOM frequencies will be controlled by proper setting of the cavity water cooling temperature. A plunger tuner, installed on one of the three large cavity equatorial ports, shall provide an additional degree of freedom in tuning the fundamental and HOM frequencies.
The proper adjustment of the fundamental frequency for variable beam loading - with different operating temperatures and plunger positions - will be performed by means of a mechanical system driven with a stepping motor which will change the cavity length (longitudinal squeezing or stretching), within the range of elastic deformation. This system can provide a fundamental tuning range of ± 200 kHz. In operation, the cavities will be automatically tuned by a regulation loop (see section 2.5.5).

2.5.3.5 Other cavity associated equipment

Four of the five small cavity equatorial ports will be equipped with monitoring RF pick-ups, three loops and one antenna. The fifth one will be used for vacuum monitoring.
A prevacuum turbomolecular pump and a UHV ion pump (≥ 120 l/s) will be installed on one of the three large cavity equatorial ports. Pressures around 1. 10^{-9} mbar are expected with an accelerating voltage of 650 kV and a cavity wall temperature up to 85 °C.
For the bakeout of the cavities, the cooling water will be heated up to 150 °C by means of portable heater units. An appropriate insulating jacket will reduce heat exchange and ensure a tight thermal stability during the bakeout or power operations. A set of sixteen thermocouples will allow to map the temperature distribution on the cavity outer surface.

2.5.4 RF power source and feeder line

Each cavity will be individually powered with a CW klystron amplifier capable to deliver more than 180 kW. The klystrons whose main characteristics and performance are summarized in Table t254_a will be provided by the firm EEV Ltd.
The klystron DC supplies for the cathode and auxiliaries (anode modulation, cathode heating, focal coils, ion pump) will be provided by the firm THOMCAST AG. The power supplies and the control system are hosted in three different cabinets which belong to a single mechanical unit, as described in Figure f254_a.
The DC power supply for the cathode is a Pulse Step Modulator (PSM) currently used for broadcast transmitters [16]. Conceptual electronic diagrams are shown in Figure f254_b. Designed for 46 kV - 7.5 A, this PSM essentially consists of 68 power modules which are connected in series and supplied through their own secondary winding from two transformers. The two transformers are shifted in phase, resulting in a 12-pulse loading of the mains with a 6-pulse rectification in the module chain. Each one of the 68 modules represents an autonomous voltage source (Us ≈ 730 V) which may be switched on/off individually by means of fast IGBT switches operating at 14 kHz. The switching sequence and pulse duration is generated and supervised by the PSM control system such that the thermal loading of all modules is distributed equally. The switching frequency can be suppressed at the output of the module chain, by means of a low pass filter.
The main PSM features (efficiency, regulation speed and accuracy, compatibility with large variation of the load impedance) well comply with the performance specifications which are

listed in Table t254_b. Moreover, the modular concept with high redundancy (up to four defective modules without performance degradation) makes it very reliable, easy to maintain and there is no need for HV crowbars.
The RF power delivered by the klystron will be fed into the cavity input coupler via a WR1800 waveguide line including monitoring directional couplers as well as a circulator to isolate the klystron from the variable (beam-loaded) cavity impedance. All these waveguide components are commercially available. The four RF plants of the SR are arranged in pairs in two diagonally opposite RF stations. Figure f254_c shows a layout of one of them.

2.5.5 Variable beam loading compensation and low level electronic system

2.5.5.1 Variable beam loading compensation

Until now we assumed a steady state regime and a matching condition at full beam current ($\Delta f = \Delta f_m$ and $\beta = \beta_m$). Numerical values of Δf_m and β_m for the SLS typical operating conditions are given in Table t253_b. While filling the storage ring, the beam loading is varying. Maintaining the reactive beam loading compensation at constant RF voltage essentially requires the use of two servo loops:

- *the frequency tuning loop* (or "slow" phase loop) which must keep constant the phase of the RF voltage in tuning the cavity fundamental frequency;
- *the amplitude regulation loop* whose task consists in regulating the cavity input power to maintain the RF voltage constant.

Generally, *a "fast" phase loop* is also needed for compensating the phase changes which result from the varying power in the amplification chain.
Since during injection the coupling factor - whose variation would not be technically easy to realize - is kept constant and equal to β_m, there will be unavoidably some reflected power. Thanks to the circulator this reflected power, P_r will be directed to a dummy load and therefore not "seen" by the klystron. Figure f255-a shows the variations of P_d, P_b, P_r and P_t for one cavity during the injection at 2.4 GeV.
When the above conditions are met, Robinson's criterion of stability for the fundamental mode is always fulfilled [17] (see Appendix 3). The stability diagram in Figure f255_b shows that for the SLS at nominal performance the stability margin is quite comfortable. As usual, the cavity will be tuned slightly below the RF source frequency (~ 1 kHz) in order to insure a sufficient stability margin at low beam current.
The low level electronic system comprising the regulation loops mentioned before (frequency, amplitude and phase) as well as the amplifier drive chain and the RF signal measurement channels will be supplied by Sincrotrone Trieste. That will be based on the system operating in ELETTRA with minor modifications for the SLS purpose as described below.

2.5.5.2 Fundamental frequency tuning loop

The tuning loop must adjust the fundamental resonant frequency to compensate the change in temperature and reactive beam loading (resistive impedance "seen" by the RF generator for any beam loading current). This is achieved in changing the cavity length within the elastic deformation range by means of a mechanical system, driven by a stepping motor which longitudinally squeezes or stretches the cavity (symmetrical deformation).
A simplified block diagram of the loop is shown in Figure f255_c. The stepping motor is controlled in closed loop with the output signal from a phase detector; this signal is proportional to the phase difference between the cavity input signal (from waveguide directional coupler, WGC2) and the cavity pick-up signal (PU1). The phase shifter in the loop path provides an adjustable offset. Appropriate control and interlocks protect the cavity from

exceeding the elastic deformation range. Besides, an input for an external interlock that can inhibit the tuning action, an output for external interlock purposes and the options of operating in open loop with local and remote control of the motor are also provided.
The main performance specifications are the following:

- tuning range : ± 200 kHz;
- tuning speed : adjustable up to 1 kHz / s;
- sensitivity : adjustable between ± 100 Hz and ± 1 kHz.

A tuning range of ± 200 kHz corresponds to a change in cavity length of ± 0.2 mm which remains in the limit of elastic deformation; it allows to handle cavity temperature variations of about ± 20 °C with a sufficient margin for the compensation of the largest beam loading effect which is less than 35 kHz (see Table t253_b). The tuning speed of 1 kHz/s is fast enough for the expected injection rates and the sensitivity of the loop will be experimentally optimised such that to avoid undue wear of the tuner.

2.5.5.3 Amplitude regulation loop

The amplitude loop must regulate the cavity accelerating voltage by controlling the drive power. A simplified block diagram of the loop is shown in Figure f255-d. A sample of the cavity voltage (from cavity pick-up, PU2) is detected and compared to the reference value; the error signal from the amplitude comparator is used to control a variable phase-free attenuator which sets the driving power. The “RF kick-off” input will be used to disable the loop during short RF interruptions that could be requested by the operator or the interlock system to dump the beam. The options for operating in open and closed loop, with local and remote control of the cavity voltage, are provided.
Modulating the klystron anode voltage - instead of the drive power - is regarded as another possible scheme of amplitude regulation. A switch is therefore implemented, as shown in Figure f255_d, in order to quickly change (during shutdown) the amplitude control mode, from drive to anode modulation, with direct setting of the drive level.
The main performance specifications are the following:

- open loop 3 dB bandwidth : adjustable up to 5 kHz;
- open loop DC gain : > 30 dB;
- output voltage stability : better than 1 %;
- recovery time (100 % modulation) : < 10 ms;
- output power dynamic : > 20 dB.

2.5.5.4 Phase regulation loop

The phase loop must compensate for the phase changes in the amplification chain with variable power. It shall also cope with the ripple coming from the klystron power supply.
A simplified block diagram of the loop is shown in Figure f255_e. The RF signals at the input and output of the amplification chain are compared in phase and the error signal is used to control an electronic phase shifter. PHS0 and PHS1 are mechanical phase shifters, driven with locally/remotely controlled motors; their variation range is 500° in steps of less than 1°. PHS1 is used to properly set the regulation point for any klystron operating conditions, while the reference phase of the plant is fixed by means of PHS0. The options for switching from open to closed loop and for disabling the loop action with an external interlock are provided.
The main performance specifications are the following:

- open loop 3 dB bandwidth : adjustable up to 5 kHz;
- open loop DC gain : > 30 dB;
- correction range : ± 30 °;
- phase stability : ± 0.5 °;

- recovery time (± 30 ° modulation): < 10 ms;
- output power dynamic : > 20 dB.

The bandwidth of both the phase and amplitude loops will be experimentally optimized to provide enough damping while remaining insensitive to the synchrotron frequency.
The combined performance of the power supplies, klystrons, phase and amplitude loops, as described before, should ensure highly stable conditions within the full SLS operating range of beam energy and current.

2.5.5.5 Drive chain

A simplified block diagram of the drive chain is shown in Figure f255_f. The signal from the 500 MHz master oscillator, after being split and phase/amplitude regulated, is amplified with a solid state 50 W drive amplifier.
A fast RF switch at the input of the chain can remove within less than 5 μs the driving RF signal under certain conditions (beam dump, klystron/cavity interlocks,…) and an output signal indicating the switch state is provided for interlock use.
A coaxial directional coupler monitors the RF signal right at the input of the klystron. The forward signal will be used to check the presence of drive power and also to protect the klystron against an overdrive. For this purpose, the rectified signal is compared to adjustable threshold values and then triggers the RF switch.
The whole drive chain shall have a 1 dB bandwidth of at least ± 10 MHz and input/output VSWR of less than 1.3 under any operating conditions.

2.5.5.6 RF signal measurements

As part of the low level electronics, measurement channels of RF signals picked up at different points of the system, are provided for monitoring purposes; they will be of three types: RF amplitude (or power), RF phase and direct RF measurements.
For the RF amplitude measurements, the rectified DC output voltage is 0 - 10 V and the accuracy better than 2 %.
For the RF phase measurements, the reference is the signal from the master oscillator. The DC output voltage is ± 10 V (for ± 180 °) and the accuracy better than 2 °.

2.5.6 RF control system

The RF control system will be produced in collaboration between THOMCAST and PSI. Its general task is to collect and process all the useful information coming from the various equipment parts in order to ensure a correct and safe (for personnel and equipment) operation of the RF system. A block diagram is shown in Figure f256_a.
The top level controller consists of a VME-bus crate operating under VxWorks and EPICS with an associated keypad and visual display. Its main functions are:

- local operator-machine interface;
- analog settings for the different equipment parts;
- command settings for the fast state machine;
- reading of the digital and analog signals;
- communication between the different VME stations (other RF plants and central SLS control system) for remote operation from the SLS main control room.

The control of the PSM is ensured by the PSM6C unit, a THOMCAST standard control and interface system which communicates with the PSM modules via fibre optic links.
The interlock protection system consists of a fast microcontroller (YCP16 from THOMCAST) and digital input/output printed circuit boards with programmable logic devices. The analog interlock inputs are converted into digital inputs by means of comparators with adjustable

thresholds. The interlock state machine controls the starting-up and switching-off sequences of the various RF equipment parts. It is realised in YCP16 and each digital interlock input/output signal has its own logic programmed locally. In this logic, it is programmed under which condition the input has to cause a fallback of the state machine and the output (action) is processed as a function of the actual state. For each interlock input, three memories are used which store the first fault event, the status of all the signals at that time and the sequence of the faults occurring afterwards (up to 9 events). The fault event and status information is available in EPICS and also indicated on the front panel of the input/output printed circuit boards by means of two-colour LED's.
The different sub-units communicate via the control and interlock bus. The output voltage of the PSM and auxiliary supplies is set from EPICS by analog 0 - 10 V control signals. Fibre optical links are used for all control signals (readings and settings) at high potential and all the other input/output signals are galvanically isolated by means of optocouplers. The relevant analog and digital signals are also available on a connector panel for debugging purposes.
This system will be integrated in the SLS central control system for remote operation from the control room; nevertheless, it shall allow a stand-alone operation of each RF plant (independently of the SLS central system). It will be hosted in an EMC-shielded control cabinet and all electrical wiring made through a filter wall (see Figure f254-a).

2.5.7 Coping with the cavity HOM

As shown from the preceding results, the RF voltage and power requirement for the SLS remain relatively modest and can be achieved using conventional equipment. The main issue certainly resides in finding an efficient means of coping with the narrow band impedances of the cavity HOM which could drive Coupled Bunch Instabilities (CBI). Both types of CBI, longitudinal and transverse, can be generated by monopole and dipole modes respectively. When exciting a mode in resonance, the growth rate of the CBI is approximately given by:

$1 / \tau_{II} = I_b \, \alpha \, f_m \, R_{II} / (2 \, Q_s \, E/e)$ in the longitudinal case;

$1 / \tau_T = I_b \, \beta_T \, f_o \, R_T / (2 \, E/e)$ in the transverse case;

f_m : HOM frequency;

R_{II} and R_T : longitudinal [Ω] and transverse [Ω/m] HOM impedance;

$Q_s = f_s / f_o$: synchrotron tune; β_T : beta-function at the cavity location.

The stability is ensured when the growth rate of the CBI is less than the radiation damping rate. From the above formulas and the expected values of cavity HOM impedances [10,18,19], one can deduce that many of the HOM whose frequency is lower than the tube cutoff frequency are susceptible to generate CBI, limiting the maximum admissible current to levels as low as a few mA.
There exist different possible cures for this problem:

a) strong de-Qing of all the HOM resonances by means of external absorbers coupled to the cavities;
b) damping of the resulting oscillations by means of active feedback systems;
c) frequency tuning of the HOM resonances away from the coupled bunch modes spectral components;
d) creating artificial (Landau) damping, for instance with a higher harmonic RF system or by partial filling of the ring.

The efficiency of the last method is relatively limited and is regarded only as a complementary means of achieving the required stability.
Solution a) implies significant complications in the cavity design and fabrication. In order to fulfill the stability conditions, it is usually combined with b) which also requires rather

complex components (broadband electronics, pick-ups, amplifiers and kickers). This is the approach followed for most of the future Meson Factories [20-23].
Solution c) which is already applied at several places, has been largely developed for the Tsukuba Photon Factory and recently improved by ELETTRA people [24]. In practice the HOM frequencies are controlled by temperature regulation of the cavity cooling water, while the fundamental mode is tuned by longitudinally squeezing/stretching the cavity. The installation of a plunger tuner provides an additional degree of freedom.
This technique of HOM tuning was preferred to the others, for the following reasons:

- it has been successfully experimented in ELETTRA with operating conditions very similar to ours;
- it does not require any special equipment on the cavities;
- it could be complemented - if necessary - by one of the methods mentioned before (a feedback system, for instance);
- it allows to switch at will between different modes of operation: a controlled excitation of the CBI is a way of trading off brightness for longer lifetime; this is applied in the "Elettra user mode" to increase the lifetime by a factor two at the expense of 20-30 % less brightness [25].

An illustration of this method, extrapolated to the SLS case, is shown in Figure f257_a. The measured longitudinal HOM parameters of one of the ELETTRA cavity, as listed in Table t257_a [26], were used for the computation of the longitudinal CBI growth rates versus the cavity temperature. The horizontal axis crosses the vertical one at a point which corresponds to the radiation damping rate (~ 200 s^{-1}). Stability is insured when the growth rate is lower than this limit. The plot of Figure f257_a shows that, within the temperature range of 40 - 70 °C, two large intervals fulfill this condition: 45 - 52 °C and 58.8 - 62 °C. Each peak represents the interaction of a HOM with a coupled bunch mode. It occurs three times - at a repetition of 1 MHz - for mode L9 which has the largest temperature coefficient and therefore determines the maximum width for a stable interval: 7.5 °C here. Modes L2, L6 and L8 are stable for any temperature while mode L1 would drive a CBI outside the operating range, at a temperature of 100 °C.
The fundamental frequency compensation for the beam loading does not dramatically modify the HOM distribution and only results in a reduction of the stable interval by a fraction of a degree.
It is worthwhile to note that this is a theoretical case, based on the use of a cavity which would be identical to the ELETTRA cavity considered here. Practically, due to the mechanical tolerances, the HOM distribution is different from one cavity to the other. *Although it is unlikely*, a configuration without any stable interval could be encountered for a specific cavity. This might happen, in particular, if mode L1 which has the largest impedance, the lowest temperature coefficient - and therefore exhibits the widest resonance - would fully interact within the operating temperature range. Such an unfavorable case, artificially created by proper modifying the HOM frequencies, is illustrated in Figure f257_b. As already mentioned, the use of a plunger aimed at shifting the frequency of mode L1 should prevent this kind of situation.
Applying the same treatment for the transverse dipole modes (Table t257_b) [26], we found that the situation was much less critical than in the longitudinal case. The stability is ensured provided that the horizontal and vertical β-functions at the cavity locations remain smaller than 0.5 m. Otherwise, resonant conditions should be easily avoidable by combining the HOM frequency control - as described before - with tune and chromaticity adjustments.
This method of dealing with the CBI requires a perfect knowledge of all the cavity mode parameters and their sensitivity to the different tuning means. A significant amount of

theoretical and experimental work was performed in this domain at ELETTRA. The use of similar cavities and tuning devices for the SLS should permit to fully take advantage of this expertise.
The cavities, like any change in vacuum chamber cross section, also contribute to the ring effective broad band impedance, Z/n which leads to HOM power losses and can drive single bunch instabilities. A value of 1 Ω is considered as a reasonable guess for $(Z/n)_0$, the low frequency limit of Z/n (see section 2.7). We estimate the contribution of the four cavities to be about 10 %. The HOM power losses should not exceed a few kW for the entire ring and a few hundreds W in one cavity.

2.5.8 Possible further upgrading

The nc system described before - while operating at relatively conservative performance levels - should be capable of fulfilling the SLS nominal requirement.
The SLS brightness could be further improved following different approaches. Unfortunately, this is generally at the expense of a strong reduction in beam lifetime (see section 2.7). Enlarging the energy acceptance with a significant increase of the RF voltage is one of the possible solutions for recovering the lifetime. Doubling the RF voltage while maintaining relaxed operating performance would require twice the number of nc cavities. Replacing the nc cavities by sc cavities would be another alternative. Instead, complementing the initial nc system with a fully idle (no external RF source) 500 MHz sc cavity is regarded as a more attractive solution.
Another method for improving the beam lifetime consists of lengthening the bunches with a higher harmonic RF system (1 or 1.5 GHz). Within this scheme, using an idle sc cavity would be also very attractive.

2.5.8.1 Superconducting RF cavities

A sc system, as compared to a nc one, has the obvious advantage of limiting the wall dissipation to a negligible amount; it also permits to reach higher accelerating gradient: 10 MV/m in a 500 MHz sc cavity is considered nowadays as a rather common performance and the higher is the frequency, the higher is the achievable accelerating gradient [38,41]. However, the minimum number of needed cavities is essentially dictated by the limitation in cavity input power: typically 100 kW for the systems already operating in other laboratories [27,28,29]. Input couplers, capable of handling higher power, are presently under development at different places [29,30,31]. Nevertheless, due to the huge ratio of beam-to-cavity power, ensuring stable operating conditions remains a critical issue and this involves the use of feedback systems [45]. The proposed hybrid “powered nc and idle sc” system, which is described in the next section should solve the power related problems and allow full profit of the sc cavity accelerating gradient.
Concerning the coupled bunch instabilities, with a sc system there is no other alternative cure than a strong de-Qing of all the cavity HOM resonances. The required amount of de-Qing for the SLS is well above the capability of the existing systems. However, there are different technical approaches presently developed for the B-Factories [29,32,33] or other Light Sources [34,35] which could be applied to the SLS.
More generally, the higher degree of complexity of a sc system makes the design, fabrication and operation more delicate. It is also worthwhile to mention that at PSI there is a lack of expertise in the various fields which are associated to the RF sc technology. The acquisition of this “new culture” together with the development program would be hardly compatible with our time schedule. For these reasons, the use for the SLS of a sc RF system as a starting solution has been ruled out. Nevertheless, we will attentively follow the developments

carried out elsewhere on the "HOM free" sc cavities in view of possible further upgrading as described next.

2.5.8.2 The hybrid "powered nc and idle sc" RF system

Detailed studies of such a system were previously reported in [36,37] for the bunch shortening case. The basic idea is to separate the functions of the two RF systems in order to optimize their respective performance: the nc system supplies the power for replacing the losses per turn; the beam-driven sc system only contributes to the potential well.

2.5.8.2.1 Beam induced voltage in an idle cavity

The power deposited by the beam passing through an idle (no external RF source) cavity is:

$$P_b = V I_b \cos\psi = - V I_b \sin\phi_s = V^2 / (2 R_s)$$

where, $V = 2 R_s I_b \cos\psi$, is the cavity voltage induced by the beam;

I_b is the beam average current; R_s is the cavity shunt impedance; $\phi_s = \psi - \pi / 2$, is the synchronous phase and ψ is the cavity tuning angle defined as : $tg\,\psi = 2 Q \delta f / f_r$ where Q is the cavity quality factor and $\delta f = h f_o - f_r$; f_o , f_r and h are the revolution frequency, the cavity resonant frequency and harmonic number, respectively. The corresponding phasor representation is shown in Figure f258_a.

One can also express the beam induced voltage as:

$$V = I_b \sin\psi (R/Q) f_r / \delta f$$

and if the cavity is detuned sufficiently far from the resonance ($\delta f >> f_r / Q$) , one gets :

$$\psi \approx \pi / 2 , \quad \phi_s \approx 0 , \quad P_b \approx 0$$

$$\text{and } V \approx I_b (R/Q) f_r / \delta f .$$

The above results point out that the induced RF voltage which is proportional to the beam current can be controlled via the cavity frequency detuning (linear dependence). Note also that the sign of the induced voltage (focusing or defocusing) depends on the direction of the detuning.

A sc cavity with its very high Q is the ideal component for making use of the induced voltage while keeping the beam energy losses at negligible level : assuming a typical R/Q value of 50 Ω * and the SLS nominal beam current (I_b = 0.4 A), one finds that 2.6 MV are induced when the cavity is detuned by about 4 kHz at 500 MHz. This amount of detuning - which corresponds to several thousands of sc cavity bandwidths (a few Hz) and remains much smaller than the revolution frequency - well fulfills the required conditions, $\delta f >> f_r / Q$. The induced voltage could be easily maintained even at extremely low current by controlling the detuning, still within the previous limit. The beam power deposited into the sc cavity, equal to the wall dissipation (~ 50 W), is negligible as compared to the radiation losses.

All the above results also apply to a higher harmonic cavity.

Obviously, an idle cavity has to be complemented with another RF system which will provide the power necessary to compensate the beam radiation losses. The beam dynamic equations for such a system are derived in Appendix 1.

2.5.8.2.2 Increase of the energy acceptance using a 500 MHz idle sc cavity

If one combines the previously described 500 MHz nc system with an idle sc cavity of same frequency, the total RF accelerating voltage "seen" by the beam can be expressed as:

$V(t) = V_T \sin(\phi(t) + \phi_s)$, where, for $\phi_{sc} \approx 0$ (idle sc cavity),

$V_T = (V_{nc}^2 + V_{sc}^2 + 2 V_{nc} V_{sc} \cos\phi_{nc})^{1/2}$ and $tg\,\phi_s = V_{nc} \sin\phi_{nc} / (V_{nc} \cos\phi_{nc} + V_{sc})$.

---

* 50 Ω is a typical R/Q value for a "HOM free" single cell sc cavity with large beam aperture [29,41].

Figure f258_b shows the RF voltages (nc, sc and nc+sc) versus phase in the SLS case with $V_{nc} = V_{sc} = 2.6$ MV; one gets for the overall RF voltage an amplitude, V_T of 5.2 MV and a synchronous phase, ϕ_s of 6.5°. The associated RF buckets (nc and nc+sc), computed from the beam dynamic equations (Appendix 1), are also shown in Figure f258_b. As compared to the initial situation with only the nc system, this corresponds to an enhancement factor of 1.6 in terms of energy acceptance. Concurrently, since the sc cavity is here detuned such as to produce additional focusing, the bunches are shortened by a factor of 1.4. Taking into account both effects, the beam life time can theoretically be improved by a factor of about 2.5 [39]. A further reduction might come from the effective lattice acceptance whose final value is expected to be slightly lower than initially anticipated [40,5].
Concerning the Robinson's criterions for the stability of synchrotron oscillations, the presence of the idle sc cavity is beneficial since it reinforces the oscillation damping strength while keeping the instability current threshold unchanged (see Appendix 3).
During the injection, the RF voltage in the sc cavity will build up with the current and the induced transients should always remain quite tolerable. Note also that, during the injection, the detuning of the sc cavity is a free parameter that can be set at will.
In the storage regime the RF voltage of the sc cavity is controlled via its frequency tuning system. The stability constraints on this voltage are relatively relaxed since it only marginally affects the beam dynamics which is essentially determined by the powered nc system.
For the operation modes where the lifetime is less critical, the presence of the sc cavity will permit to save a significant amount of the power dissipated in the nc cavities by operating them at reduced voltage and larger synchronous phase.

2.5.8.2.3 Lengthening of the bunches using a 2nd or 3rd harmonic idle sc cavity

An alternative method of improving the beam lifetime consists in producing longer bunches with less density. Again, this could be advantageously realized using a hybrid system as described before but with a higher harmonic cavity detuned in the other direction (de-focusing case). Figure f258_c shows the RF voltages (nc, sc and nc+sc) versus phase, as well as the associated RF buckets and bunch profiles, in the SLS case with a 2nd harmonic (1 GHz) idle sc cavity. The beam induced voltage of about 1.2 MV, required to have a quasi zero slope over the phase domain covered by the bunch, is obtained with a detuning of 16 kHz (for $R/Q \approx 50\ \Omega$, as before). One finds that the bunches are lengthened by a factor of about four ($\sigma_z \approx 4.\sigma_{zo} \approx 15$ mm), the energy acceptance is nearly unaffected and the phase acceptance is even enlarged as compared to the single nc system. Consequently, the beam lifetime should be improved by about a factor four as the bunch length. Although the phase acceptance is slightly reduced, quite similar results are obtained with a 3rd harmonic system (see Figure f258_d). The required voltage of about 0.85 MV at 1.5 GHz is obtained for a detuning of 36 kHz, again assuming a R/Q of 50 Ω.
Concerning the Robinson stability, the condition is more delicate than in the focusing case since the harmonic sc cavity is now detuned such that it contributes to anti-damping. However, provided that its resonant frequency is not set in a way presenting a too high impedance at the first satellites of the synchrotron frequency (side-bands), the overall effect should be dominated by the damping coming from the nc system. In principle, this is not a critical issue since the sc cavity naturally has an extremely narrow bandwidth (see Appendix 3).
Although the required performance is fully compatible with the use of a single sc cavity, adding a second one could present significant advantages:

- lower accelerating gradient and cryogenic losses for the same voltage;
- higher voltage capability;

- extension of the operating beam current range down to lower values (doubled detuning for the same voltage and current);
- possibility of applying the two-cavity HOM damping technique developed for SOLEIL [35]; as mentioned before, for coping with the HOM, different approaches could be adopted.

The previous results tend to demonstrate that, in order to improve the SLS beam life time, the bunch lengthening technique is more efficient than increasing the fundamental RF voltage. Moreover, with the former solution, one can expect a significant amount of Laudau damping - due to the nonlinearity of the RF waveform - which should help in fighting the coupled bunch instabilities. Another benefit is that the resulting decrease in peak current should raise the threshold for single bunch instabilities. Note also that the harmonic cavity could easily be detuned in the other direction shortening the bunches by a factor 1.5, if needed. Furthermore, one could cumulate the benefits of both methods in implementing three idle sc cavities: one 500 MHz and two harmonic cavities. The beam life time would then be theoretically improved by an order of magnitude or alternatively, the bunches shortened by a factor two.

Idle harmonic nc cavities are also being operated in other laboratories [42]. Applied to the SLS case, this solution would require about ten cavities in order to keep at a reasonable level the amount of power to be restored by the main RF system and ensure safe conditions for Robinson's stability (see Appendix 2 and 3). An effective cure to the HOM impedances would have to be found as well and that could be the tuning technique which is used for the 500 MHz system. An alternative idle nc system for the SLS is described in Appendix 3 and the main features of the two versions are compared in Table t258_a. Although the sc option appears to be more convenient, the idle nc system remains a possible alternative for the bunch lengthening application. Further investigations are needed for weighting up the respective advantages and drawbacks of the nc and sc versions.

2.5.9 Conclusions

The nominal RF power and voltage requirement for the SLS storage ring are quite modest and achievable with conventional, already well-proven equipment that can be available and operational within relatively short times. It is planned to use four 500 MHz plants, each consisting of a nc single cell cavity similar to that used in ELETTRA, powered with a 180 kW CW klystron amplifier via a WR1800 waveguide line. The cavity input coupler is of the coaxial type, terminated by a coupling loop. For coping with the cavity HOM impedances, the parasitic frequencies will be detuned to avoid resonant excitations by the beam. This can be achieved by combining three tuning means: temperature control of the cooling water, elastic mechanical deformation and a plunger tuner. In addition, each plant will be equipped with standard amplitude and phase regulation loops.

This system - while operating at relatively conservative performance levels - should be capable of fulfilling the SLS nominal requirement.

The use of superconducting cavities has been ruled out as a starting solution. However, for improving the beam lifetime the initial nc system could be further complemented with idle (no external power source) sc cavities. Within this scheme, the beam power is entirely supplied by the nc system while one takes full profit of the beam induced voltage in the sc cavities. Such a system could be used either to double the fundamental RF voltage with one 500 MHz sc cavity, or to lengthen the bunches by a factor three to four with one (possibly two) 2nd / 3rd harmonic sc cavity (ies). The computer simulations indicate that the latter solution would be more efficient for our purpose. Furthermore, we could cumulate the benefits of both methods in implementing three idle sc cavities: one 500 MHz and two harmonic cavities. This would

theoretically result in improving the beam life time by about one order of magnitude and alternatively offer the possibility of shortening the bunches by a factor two.
A priori, the *hybrid "powered nc and idle sc" system* should not pose any special problem. On the contrary, it appears to be particularly flexible and easy to control; moreover, the difficulties related to the transmission of large power through the sc cavities and the associated technological problems are eliminated. The main challenge for the use of a sc cavity in such a high current machine certainly resides in the damping of the parasitic HOM impedances which can drive coupled bunch instabilities. Programs of development aimed at solving this problem, have been launched at several laboratories. We will attentively follow their advancement in view of a possible application in the SLS.
For the bunch lengthening purpose, an idle 3rd harmonic nc system (~ 10 cavities) remains an attractive alternative. Further investigations are necessary for weighting up the respective advantages and drawbacks of the sc and nc versions.

2.5.10 References

[1] P. Marchand, RF for Synchrotron Radiation Sources (1.5-2.5 GeV), SLS-Note 6/95, presented at the first RF Workshop of the New European Light Source Projects, Karlsruhe Research Center, October 1995.
[2] P. Marchand, RF system for the SLS, PSI SLS Note 14/96, September 1996.
[3] P. Marchand, RF System for the SLS Booster and Storage Ring, PSI Note SLS-TME-TA-1998-0011, September 1998.
[4] P. Marchand, Use of an idle superconducting cavity for improving the energy acceptance in the SLS storage ring, PSI SLS Note 19/96, October 1996.
[5] J. Bengtsson et al, Increasing the energy acceptance of high brightness synchrotron light storage ring, NIM A404, p. 237-247, 1998.
[6] P. Marchand, Foils of the SLS MAC meeting, December 1996 and Presentation at the 4th RF workshop of the New European Light Source Projects, Daresbury, UK, April 1997.
[7] P. Marchand, Possible upgrading of the SLS RF system for improving the beam lifetime, PSI Note SLS-TME-TA-1998-0012, September 1998.
[8] M. Böge et al, The Swiss Light Source Accelerator Complex: An Overview, presented at the EPAC98, Stockholm, June 1998.
[9] A. Fabris and M. Svandrlik, private communication.
[10] F. Perez, Comparative Study of Cavities for the LSB, LSB/RF/01/96, 01-05-96.
[11] P.A. McIntosh, Preliminary Investigations of an RF Cavity for Diamond, DIAMOND/RF/95/01, September 1995.
[12] H.O. Moser et al, Vorschlag zum Bau einer Synchrotronstrahlungsquelle (ANKA) im Forschungszentrum Karlsruhe zur Förderung der industriellen Umsetzung von Mikrofertigungs- und Analytikverfahren, Forschungszentrum Karlsruhe, September 1995.
[13] P. Marchand, Design of the RF accelerating system for the storage ring of the B-Meson Factory proposed at PSI, PSI-TM-12-89-04.
[14] A. Massarotti et al, 500 MHz Cavities for the Trieste Synchrotron Light Source ELETTRA, Proceedings of the EPAC90, Nice, France, p. 919-921, June 1990.
[15] S. Voigt et al, Leistungstest der ELETTRA-Einkopplung, Versuchprotokoll PSP Nr : 1.0600, Forschungszentrum Karlsruhe, March 1997.
[16] THOMCAST AG, Brief Description of the Pulse-Step Modulator TSM 6, TSM6_E.PM5, September 1996.
[17] K. Robinson, CEA-II (1956) and CEAL 1010 (1964).
[18] A. Karantzoulis et al, Observation of Instabilities in the ELETTRA Storage Ring, Proceedings of the EPAC94, p. 119-121, London, June 1994.

[19] P. Marchand, The Collective Phenomena in the B-Meson Factory Storage Ring proposed at PSI, PSI-TM-12-89-05, July 1989.
[20] M. Zobov et al, Collective Effects and Impedance Study for the DAΦNE Φ-Factory, LNFN-95/041 (P), July 1995.
[21] H. Schwartz and R. Rimmer, RF System Design for the PEPII B-Factory, Proceedings of the EPAC94, p. 1882-1884, London, June 1994.
[22] T. Kageyama et al, Design of a Prototype of RF Cavity for the KEK B-Factory (KEKB), Proceedings of the EPAC94, p. 2098-2100, London, June 1994.
[23] P. Marchand, RF System for High Luminosity e+ e- Colliders, Proceedings of the EPAC90, p. 1088-1090, Nice, June 1990.
[24] M. Svandrlick et al, Improved Methods of Measuring and Curing Multibunch Instabilities in ELETTRA, presented at the EPAC96, Sitges, Spain, June 1996.
[25] A Wrulich et al, Observation of Coupled Bunch Instabilities in ELETTRA, presented at the EPAC96, Sitges, Spain, June 1996.
[26] M. Svandrlick et al, Simulations and Measurements of Higher Order Modes of the ELETTRA RF Cavities in view of Coupled Bunch Instability Compensation by Temperature Variation, presented at the EPAC96, Sitges, Spain, June 1996.
[27] B. Dwersteg et al, Operating Experience with Superconducting Cavities in HERA, Proceedings of the EPAC94, p. 2039-2041, London, June 1994.
[28] S. Noguchi et al, Recent Status of the TRISTAN Superconducting RF System, Proceedings of the EPAC94, p. 1891-1893, London, June 1994.
[29] J. Kirchgessner, Review of the Development of RF Cavities for High Currents, Proceedings of the IEEE PAC, p. 1469-1473, Dallas, May 1995.
[30] M. Pisharody et al, High Power Window Tests on a 500 MHz Waveguide Window for the CESR Upgrade, Proceedings of the IEEE PAC, p. 1720-1722, Dallas, May 1995.
[31] J. Tückmantel et al, Improvements to Power Couplers for the LEP2 Superconducting Cavities, Proceedings of the IEEE PAC, p. 1642-1644, Dallas, May 1995.
[32] T. Tajima et al, Development of HOM Damper for B-Factory (KEKB) Superconducting Cavities, Proceedings of the IEEE PAC, p. 1469-1473, Dallas, May 1995.
[33] W. Hartung et al, Measurement of the Interaction between a Beam and a Beam Line Higher-Order Mode Absorber in a Storage Ring, Proc. of the IEEE PAC, p. 3294-3296, Dallas, May 1995.
[34] A. Fabris et al, Design of a 3rd harmonic superconducting cavity for bunch lengthening in ELETTRA, presented at the EPAC98, Stockholm, June 1998.
[35] A. Mosnier et al, HOM damping in SOLEIL superconducting cavity, presented at the EPAC98, Stockholm, June 1998.
[36] P. Marchand, Hybrid Normalconducting / Superconducting RF System for High Luminosity Circular e+ e- Colliders, Particle Accelerators, Vol 36, Numb. 1-3 (1991), p. 205-222, March 1991.
[37] P. Marchand and L. Rivkin, Idle Superconducting RF Cavities for Bunch Focusing, Proceedings of the IEEE PAC, p. 780-782, San Francisco, May 1991.
[38] E. Kako et al, Thermal quench on the 1.3 GHz high gradient superconducting cavities, Proceedings of the EPAC96, p. 2124-2126, Sitges, Spain, June 1996.
[39] P. Marchand, SLS: beam lifetime and bunch lengthening versus RF voltage, PSI SLS-Note 17/96, October 1996.
[40] A. Streun, Momentum acceptance and Touschek lifetime, PSI SLS Note 18/97, November 1997.
[41] T. Furuya et al, A prototype module of a superconducting damped cavity for KEKB, Proceedings of the EPAC96, p. 2121-2123, Sitges, Spain, June 1996.

[42] A. Anderson et al, Landau cavities at MAX II, presented at the EPAC98, Stockholm, June 1998.
[43] R.A. Rimmer et al, A third-harmonic RF cavity for the Advanced Light Source, presented at the EPAC98, Stockholm, June 1998.
[44] P. Marchand, Robinson's stability criterion for narrow band resonators in large accelerators and storage rings, CERN/EF/RF 84-5, July 1984.
[45] A. Mosnier, RF feedback systems for sc cavities, presented at the EPAC98, Stockholm, June 1998.

Appendix 1

Beam dynamic equations for a double RF system

In presence of two RF systems, an electron at phase ϕ - with respect to the synchronous electron - experiences an overall RF accelerating voltage that can be expressed as:

$$V(\phi) = V_1 [\sin (\phi + \phi_{s1}) + a \sin (k\phi + k\phi_{s2})],$$

where V_1, $V_2 = aV_1$, $h_1 = h$, $h_2 = kh$, ϕ_{s1}, ϕ_{s2} are the peak accelerating voltage, the harmonic number and the synchronous phase for each system, respectively.

In the particular case of the hybrid "nc powered and sc idle" system one gets:

$$\phi_{s2} = \phi_{sc} = 0,\ \phi_{s1} = \phi_{nc},\ V_1 = V_{nc} \text{ and}$$

$$V(\phi) = V_{nc} [\sin (\phi + \phi_{nc}) \pm a \sin (k\phi)],$$

where the sign of the 2nd term depends on which direction the sc cavity is detuned (focusing or defocusing).

The electron synchrotron motion can be derived from the Hamiltonian as follows:

$$d\phi / dt = \delta H / \delta W, \quad dW / dt = - \delta H / \delta \phi$$

where $H(W, \phi) = (h \alpha \omega_o^2 W^2) / (2 E) + e P(\phi) / (2 \pi)$,

$$P(\phi) = - \int_0^{\phi} [V(\phi) - V(0)] d\phi ,$$

$W = \Delta E / \omega_o$,

ΔE is the electron energy deviation,

$\omega_o = 2 \pi f_o$,

and the other parameters are defined in Table t252_a.

Since the electron trajectories in the longitudinal phase space (ϕ, W) are contours of constant Hamiltonian, one can compute from the above equations the boundary of the stable region ("RF bucket"), the energy and phase acceptance as well as the equilibrium bunch profile which is given by:

$$I (\phi) = A \exp [P(\phi) / (V_1 \sigma_{\phi o}^2 \cos \phi_{s1})],$$

where A is the normalization constant and $\sigma_{\phi o}$ is the RMS bunch length (in RF phase unit) when only the first system is active ($V_2 = 0$).

It is worthwhile to note that the product of the bunch length and the synchrotron frequency remains constant for any value of the overall RF voltage:

$$\sigma_{\phi o} f_{so} (@\ V_2 = 0) = \sigma_{\phi} f_s, (@ \text{ any value of } V_2).$$

The above theory is still applicable to the bunch lengthening case - with nonlinear RF waveform - as far as the RF voltage slope is not too much distorted within the phase domain covered by the bunches; that is valid for the numerical examples shown in Figures f258_c and f258_d. The effect of strong non-linearity on the bunch shape becomes visible if the slope of the RF voltage at the bunch location approaches too much zero, as illustrated in Figure f258_e. The electron distribution within the bunches is then largely distorted and extremely sensitive to the variations of the RF voltage.

Appendix 2

Harmonic idle nc system for bunch lengthening

For the nc version, we chose a 3rd harmonic system (f_r = 1.5 GHz) that is a quite good compromise between shunt impedance, ratio of wave length over bunch length and equipment size.

The main requirements for the design of the system are the following:

1) the maximum power lost by the beam and to be restored by the main 500 MHz RF system must not exceed P_{max} = 40 kW;
2) the derivative of the overall voltage must be close to zero at the bunch phase;
3) the RF wave-form should not present too much non-linearity over the phase range covered by the bunches;
4) the Robinson stability should be ensured for the overall system;
5) the four above conditions must be fulfilled for a stored beam current, I_b ranging between 0.15 A and 0.4 A.

The beam induced voltage and power lost in an idle RF system are (see section 2.5.8.2.1):

$$V = 2 R_s I_b \cos\psi = I_b \sin\psi \, (R/Q) \, f_r / \delta f$$

$$P = V I_b \cos\psi = - V I_b \sin\phi_s = V^2 / (2 R_s).$$

Combining the above equations with requirements 1) and 2) leads to:

$$\text{tang}\,\psi = 2Q \, \delta f / f_r \geq I_b V_1 \cos\phi_{s1} / (k P_{max}),$$

$$V \geq P_{max} / (I_b \cos\psi),$$

$$R_s \geq V^2 / (2 P_{max}).$$

Applied to the SLS case, one finds that the required shunt impedance is about 10 MΩ and then, with this value, conditions 3) and 4) are also satisfied for operation at the full beam current of 0.4 A. Besides, the stability analysis (see Appendix 3) pointed out that another constraint was requirement 4) at the lowest stored beam current: a R/Q value of about 600 Ω is necessary to ensure a stable operation at 0.15 A.

In practice, this could be achieved using 10 pill-box cavities similar to that used at MAX II (R/Q ≈ 65 Ω, Q ≈ 15000) [42]. With nose-cone type cavities optimised for higher impedance as in ALS [43], one could reduce the number of required cavities down to 8. In order to cure the HOM problem, the temperature tuning technique could be applied as for the 500 MHz system.

Typical operating parameters for such a system are listed in Table t258_a and compared to the sc version. The nc system presents a few drawbacks:

- large number of cavities;
- significant amount of power to be restored by the 500 MHz system;
- any variation of current or cavity frequency leads to a change in power loss which is directly reflected back to the 500 MHz system; troubles could possibly result from this coupling between the two systems through the beam;
- making the harmonic system “invisible for the beam” requires an unpractical amount of detuning;
- slight degradation of the energy acceptance.

These inconveniences are eliminated when using sc cavities.

Appendix 3

Robinson stability for a double RF system

The condition for the stability of coherent electron bunch synchrotron oscillations in the presence of a single accelerating RF system was first derived by K. Robinson [17]. The so-called "Robinson's criterion" consists in fact of two stability conditions that can be expressed:

a) $i_b < 2 V \cos \phi_s / (R_s \sin 2\psi)$;

b) $\psi > 0$;

where i_b is the Fourier component of the beam current at the RF frequency (twice the DC component for short bunches), ϕ_s is the synchronous phase; ψ, V, Rs are the cavity tuning angle, peak RF voltage and effective shunt impedance, respectively.

It is easy to verify that the two stability conditions are naturally fulfilled if the RF system is matched for maximum beam loading: $\Delta f = \Delta f_m$ and $\beta = \beta_m$ (see section 2.5.2 and Table t253_b). Figure f255_b shows a stability diagram, computed from the above relations, for the SLS 500 MHz system at nominal performance. As expected, the stability is always ensured and moreover, the stability margin is quite comfortable.

The extension of the Robinson's criterion to a double RF system [36] pointed out that the current limit given by a) is unchanged when adding an idle cavity or, in other words, the first Robinson's stability criterion is automatically fulfilled for the overall system provided that it is fulfilled for the powered system. This can be interpreted as follows: the restoring force for *coherent* phase oscillations is proportional to the slope of the *RF generator voltage* at the bunch phase (negative for stability); the inequality a) is simply an expression of this condition and consequently it is unaffected by the presence of an idle cavity. Obviously the powered system has to restore the losses in the idle system and the phase, ϕ_s corrected accordingly. While losses are negligible in sc cavities, they can become significant in nc cavities and the resulting phase change may lead to a critical reduction of the stability margin.

Requirement b) means that the detuning must be such as to provide oscillation damping, a condition which is strictly valid for a single system and when neglecting the other sources of damping (radiation damping, Landau damping, …). An idle cavity, detuned in the direction for focusing, naturally contributes to damping and conversely to antidamping for bunch lengthening. In the latter case, the stability will be ensured if the damping from the powered system compensates the antidamping from the idle system. Therefore, the resonant frequency of the harmonic system must not be set so that it presents a too high impedance at the first satellites of the synchrotron frequency ($m*f_s$).

A computer code was written for evaluating the overall damping or growth rate factors in the presence of two RF systems. The computed data are listed in Table t258_b, for the SLS case with a 3rd harmonic idle system operating in the bunch lengthening regime. These results correspond to the nc and sc versions, as described in Table t258_a. Note that the incoherent synchrotron frequency of 2.2 kHz assumed here corresponds to a bunch lengthening factor of about 3.5. One can see that in both cases the net effect at the significant side bands is a damping and when antidamping starts for higher values of m, the instability growth rate is lower than the radiation damping rate by several orders of magnitude. The stability is easily ensured in both cases with full stored beam current. Although the conditions become less favorable - especially for the nc system - when maintaining the same voltage at lower stored

beam current (smaller detuning), the stability is always ensured down to 0.15 A* . Below this value, in the nc case the growth rate of modes m = 1 and m = 2 approaches the radiation damping rate. In the sc case, the resonant excitation of one side-band could lead to trouble, even at relatively large values of m; on the other hand, due to the extremely narrow bandwidth, this is easy to avoid: changing the cavity frequency by a fraction of a kHz should be sufficient to re-establish stable conditions without affecting too much the operating parameters.
We assumed here - as usually - that the instability growth rate was proportional to the real part of the impedance. While this is certainly valid for the nc case, it could be slightly different for a sc cavity of very high Q, due to a possible "broadening process" as described in [44]. This effect - which in principle shall act favorably - should not affect too much the preceding results.
Note that the addition of a second sc cavity would improve the conditions for the operation at reduced beam current (doubled detuning at same voltage and current) and also offer a few other advantages (see section 2.5.8.2.3).

* Provided that the R/Q value is larger than 600 Ω in the nc case.

Revolution frequency, f_o [MHz]	1.04	
Momentum compaction, α	7. E-4	
Beam current, I_b [A]	0.4	
Energy, E [GeV]	2.4	
Radiation loss / turn, ΔU [MeV]	0.6	
Momentum spread, σ_p [%]	0.09	
Longitudinal damping time τ_s [ms]	4.5	
Transverse damping times, $\tau_x \approx \tau_y$ [ms]	9.	
RF frequency, f_{RF} [MHz]	499.652	
Harmonic number, $h = f_{RF} / f_o$	480	
RF power into the beam, P_b [kW]	240.	
RF voltage, V_{RF} [MV]	2.0	2.6
Overvoltage, q	3.3	4.3
RF acceptance, ε_{RF} [%]	± 3.0	± 3.7
Bunch length, σ_s [mm]	4.4	3.8
Synchrotron frequency, f_s [kHz]	6.8	7.8
Synchrotron tune, $Q_s = f_s / f_o$ [E-3]	6.5	7.5
Synchronous phase, ϕ_s [degree]	17.5	13.3

Table t252_a: Basic parameters for the SLS storage ring.

Resonant frequency, f_r	499.652 MHz
Shunt impedance, R_s	3.4 MΩ
Quality factor, Q_o	40000
Accelerating RF voltage, V_{RF}	650 kV
Power dissipation, P_d	65 kW

Table t253_a : Main cavity parameters.

I_b [mA]	V_{RF} [MV]	P_d (1c) [kW]	P_b (1c) [kW]	P_t (1c) [kW]	β_m	Δf_m [kHz]	nb of cav.
400.	2.0	37.	60.	97.	2.6	32.	4
400.	2.6	60.	60.	120.	2.0	27.	4
400.	2.0	65.	80.	145.	2.2	24.	3

Table t253_b : SLS possible operating conditions with 4 or 3 (out of 4) nc cavities in use.

- V_{RF} is the accelerating voltage "seen" by the beam (transit time factor included);
- P_d (1c), P_b (1c) and P_t (1c): wall dissipation, power delivered to the beam and total RF power per cavity;
- β_m, Δf_m : optimum coupling factor and detuning (zero reflected power at full beam current).

Frequency	499.652 MHz
1dB bandwidth (minimum)	± 1 MHz
RF nominal output power	> 180 kW
RF operating power	150 kW
Efficiency at 150 kW	> 60%
Tolerable load VSWR (all phases) at 180 kW	> 1.3
Duty cycle	cw
Output power dynamic	35 dB
Harmonic content	< - 30 dBc
Spurious and sideband level	< - 60 dBc
Signal to noise ratio within bandwidth	> 60 dB
Saturated drive power at 150 kW	< 25 W
Continuous collector dissipation capability	> 300 kW
RF phase variation vs. output power for full drive modulation	< 20°
RF phase variation over beam voltage variation for fixed modulation anode voltage	< 10°/ 1%
Variation of RF output power over beam voltage in saturated drive	< 0.1 dB / 1%
RF phase variation over cathode current	< 12° / A
Klystron input VSWR	< 1.5
Maximum RF radiation	0.1 mW/cm²
Maximum X-ray emission	0.1 μSv/h
Max. permissible energy in HV breakdown	35 J
Cathode potential for 150 kW output power	< 42 kV
Maximum operational cathode voltage	46 kV
Maximum modulating anode current	5 mA

Table t254_a : Main klystron characteristics and performance.

Parameter	*Specification*	*Note*
Voltage	0 - 46 kV	negative voltage
Current	0 - 7.5 A	
Efficiency	> 97%	
Voltage accuracy (better than)	1%	
Voltage ripple (less than)	1% pp 75 V rms 15 V rms 3 V rms 50 V rms	overall 1 kHz to 2 kHz 2 kHz to 4 kHz 4 kHz to 12 kHz above 12 kHz
Speed	1 ms	
Voltage overshoot	< 5%	under any load condition
Energy into klystron arc	< 15 J	max. 70 V arc voltage
Input voltage	400 V ± 5%	3-phase 50 Hz
Tolerable mains 3-phase asymmetries	5%	voltage drop on one line

Table t254_b : Main specifications for the klystron DC supply.

HOM	f_m (48 °C) [MHz]	R/Q [Ω]	Q	R_s [kΩ]	τ_m [kHz/°C]	φ_m
L1	949.506	28.8	35300	1017	- 11.5	0.63
L2	1057.199	0.7	33700	24	-19.3	-0.31
L3	1421.456	5.0	39300	197	-43.1	-2.16
L4	1514.638	4.9	17400	85	-28.2	-0.31
L5	1606.348	9.1	18100	165	-41.6	-2.33
L6	1876.971	0.3	41100	12	-33.4	-0.14
L7	1948.475	1.8	33100	60	-51.2	-2.23
L8	2072.036	0.1	12500	1	-110.9	-8.94
L9	2124.792	7.7	27000	208	-111.4	-9.3

Table t257_a : Measured longitudinal HOM parameters of the ELETTRA cavity [26];
τ_m is the HOM frequency temperature dependence with the fundamental mode frequency kept constant by mechanical deformation;
φ_m is the ratio of HOM - to - fundamental frequency variation.

HOM	f_m (48 °C) [MHz]	$(R/Q)_T$ [Ω/m]	Q	R_T [kΩ/m]	τ_m [kHz/°C]	φ_m
T1H	743.169	72.5	40000	2.9	-36.3	-3.1
T1V	743.303	72.7	39900	2.9	-36.0	-3.1
T2H	745.280	246.5	35300	8.7	-13.5	0.0
T2V	746.463	245.9	36200	8.9	11.5	0.0
T3H	1114.274	301.9	37100	11.2	-18.5	0.2
T3V	1114.706	304.2	35500	10.8	-16.1	0.5
T4H	1241.307	118.0	17800	2.1	-49.7	-4.0
T4V	1242.237	118.0	17800	2.1	-49.7	-3.9
T5H	1304.432	8.6	23200	0.2	-38.9	-2.3

Table t257_b : Measured transverse HOM parameters of the ELETTRA cavity [26];
τ_m and φ_m are defined as in Table t257_a;
TiH / TiV correspond to the horizontal / vertical polarizations for dipole mode i.

	idle nc sytem	idle nc system
f_r	1.5 GHz	1.5 GHz
n_{cav}	8 - 10	1
$R_s * n_{cav}$	10 MΩ	7.5 GΩ
Q_o	15000 - 20000	1.5 E8
V	0.85 MV	0.85 MV
P_d	36 kW*	50 W
I_b	0.4 A	0.4 A
ϕ_s	6 °	~ 0 °
δf	470 kHz	35.3 kHz
ε_{RF}	3.45 %	3.65 %
σ_z	15 mm	15 mm
f_s	2.2 kHz	2.2 kHz

Table t258_a

3rd harmonic idle RF system for bunch lengthening: typical operating parameters (nc and sc versions).

* Power to be restored by the 500 MHz system ($\Delta\phi_s$ of 2°).

mode number ($m*f_s$)	τ_{nc} / τ_{rad} (@ I_b = 0.4 A)	τ_{sc} / τ_{rad} (@ I_b = 0.4 A)	τ_{nc} / τ_{rad} (@ I_b = 0.15 A)	τ_{sc} / τ_{rad} (@ I_b = 0.15 A)
m = 1	D	D	D	D
m = 2	D	D	0.3	D
m = 3	3.5 E -3	D	0.1	D
m = 4	8 E - 4	D	6 E - 3	3 E - 4
m = 5	4 E - 5	5 E - 7	3 E - 4	5 E - 5

Table t258_b

Ratio of the instability growth rates over the radiation damping rate for the nc and sc cases as defined in Table t258_a at two values of the beam current (“D” is for Damping).

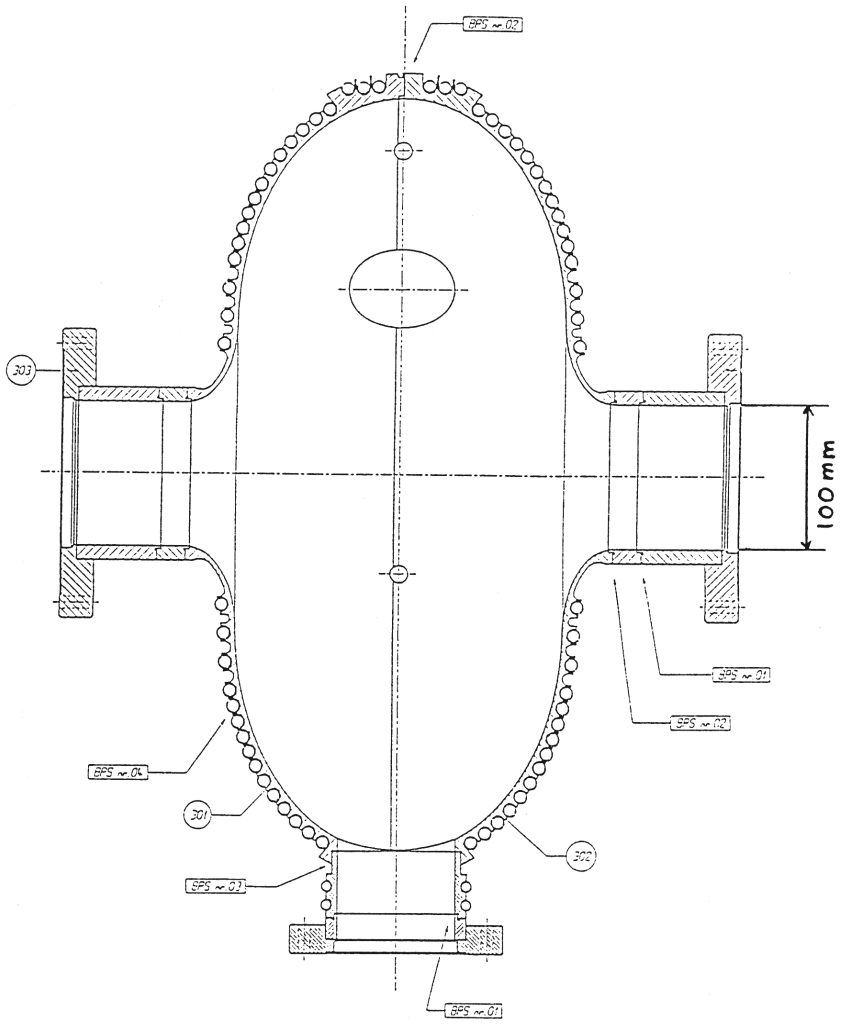

Figure f253_a : Cross section of the ELETTRA cavity.

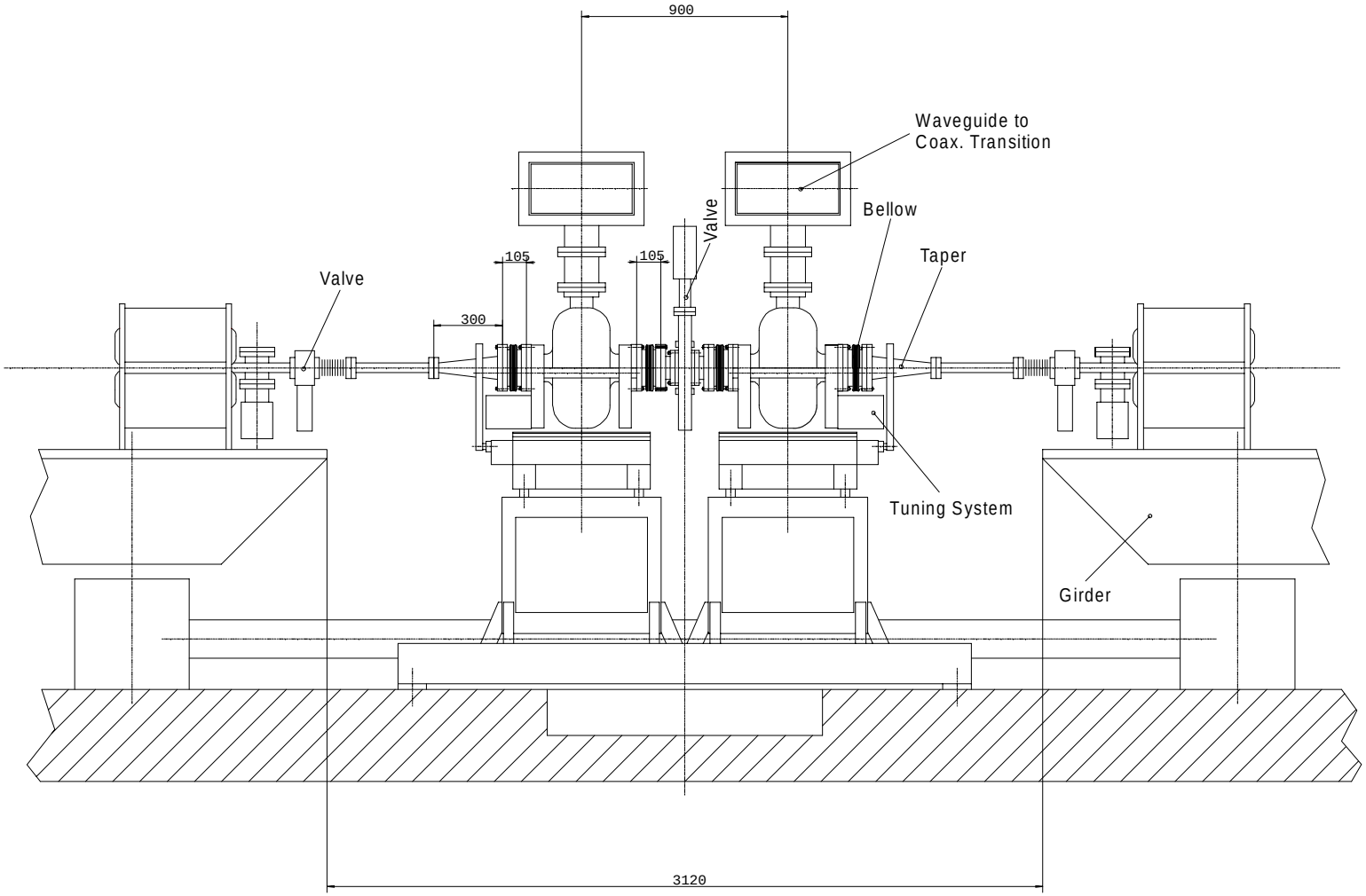

Figure f253_b : Cavity layout in the storage ring.

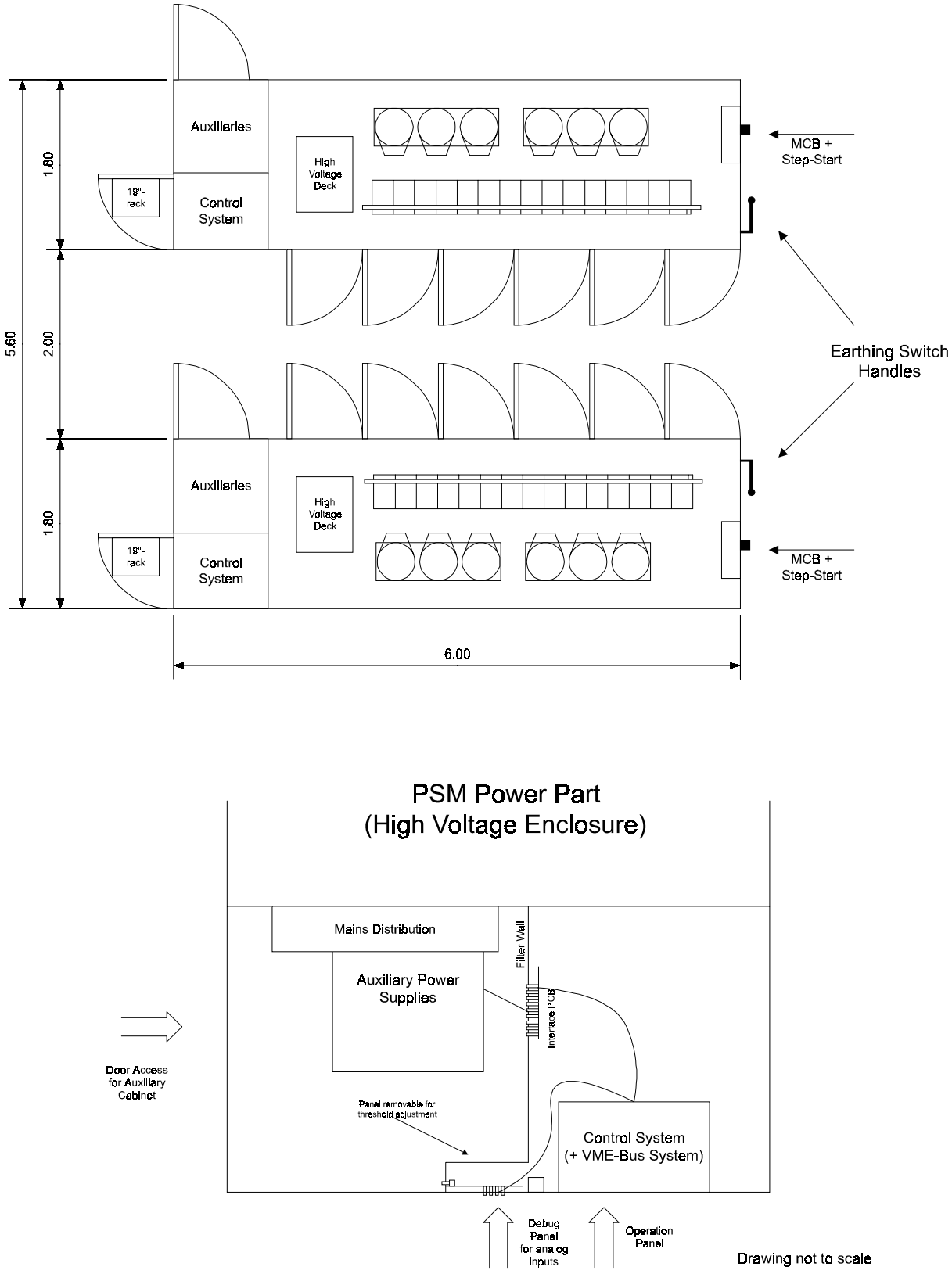

Figure f254_a : Power supply and control system cabinets.

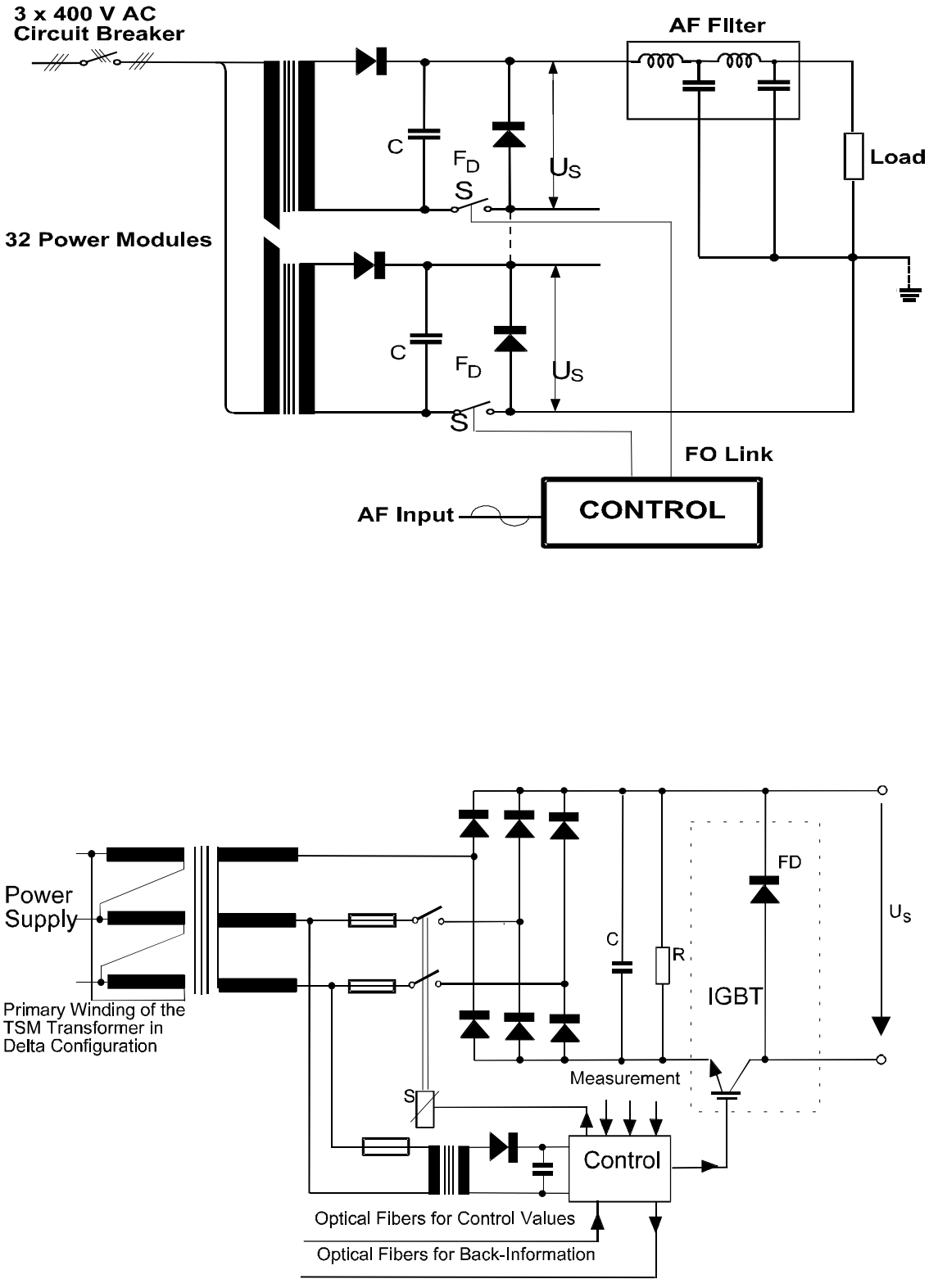

Figure f254_b : Conceptual electronic diagrams of the klystron high voltage power supply (Pulse Step Modulator from THOMCAST AG).

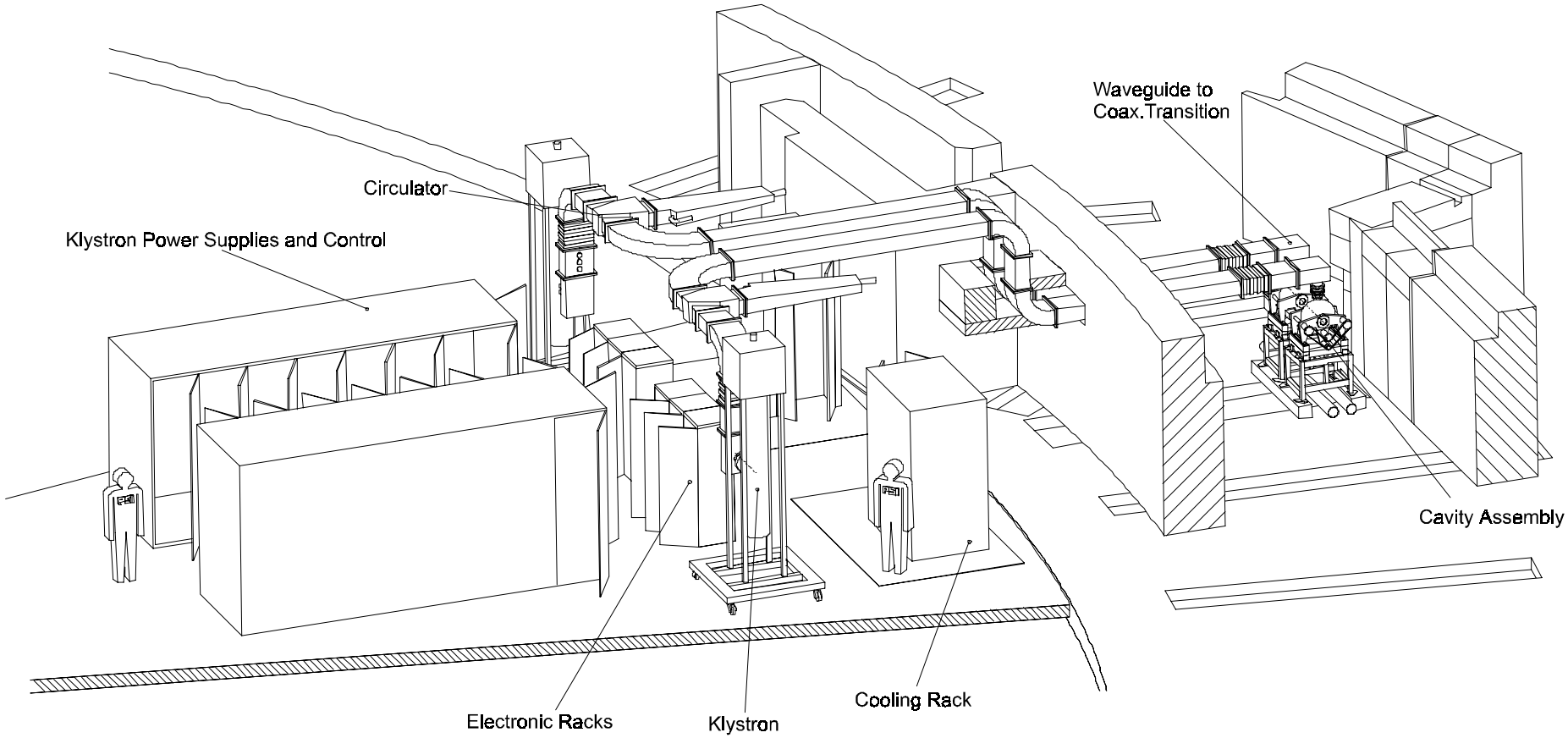

Figure f254_c : Storage ring RF station.

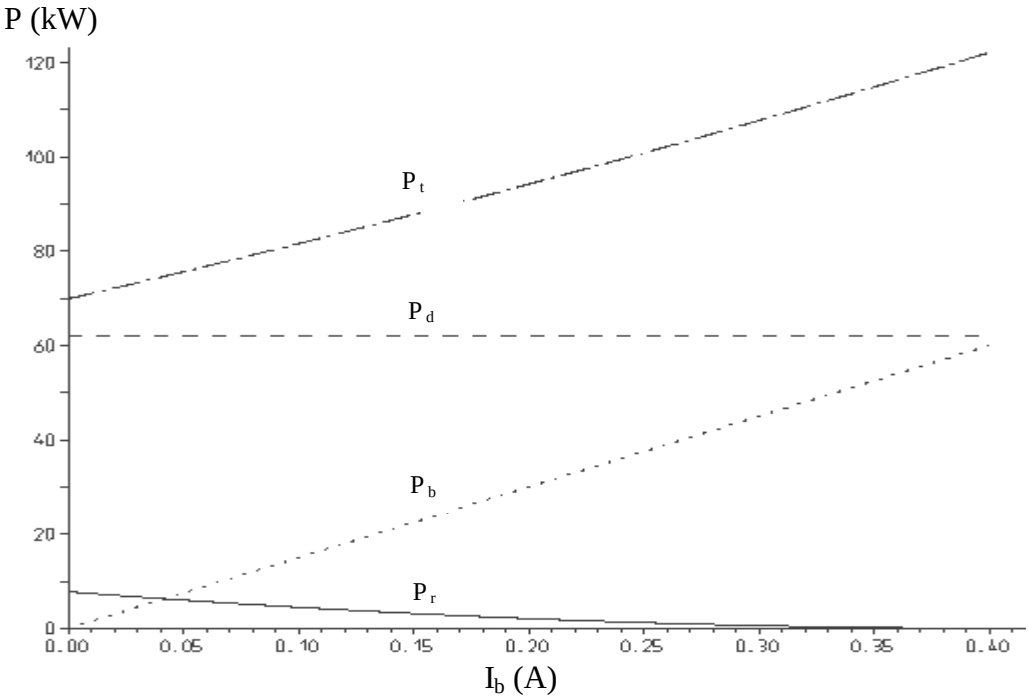

Figure f255_a : Wall dissipation (P_d), power delivered to the beam (P_b), reflected power (P_r) and total power (P_t) for one of the four SLS storage ring cavities during injection at 2.4 GeV (V_{RF} = 2.6 MV, β = 2).

$$P_t = \frac{(1+\beta)^2}{4\beta} P_d \left(1 + \frac{P_b}{P_d(1+\beta)}\right)^2 ;$$

$$P_r = P_t - (P_b + P_d) .$$

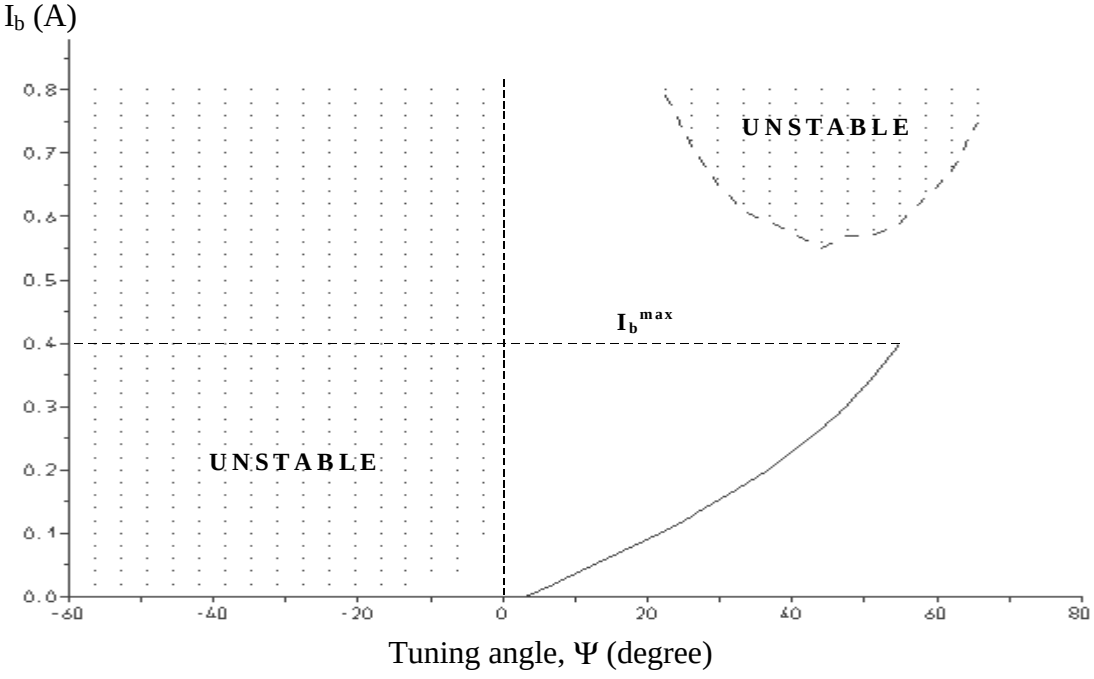

Figure f255_b : Robinson's stability diagram for the same conditions as above.

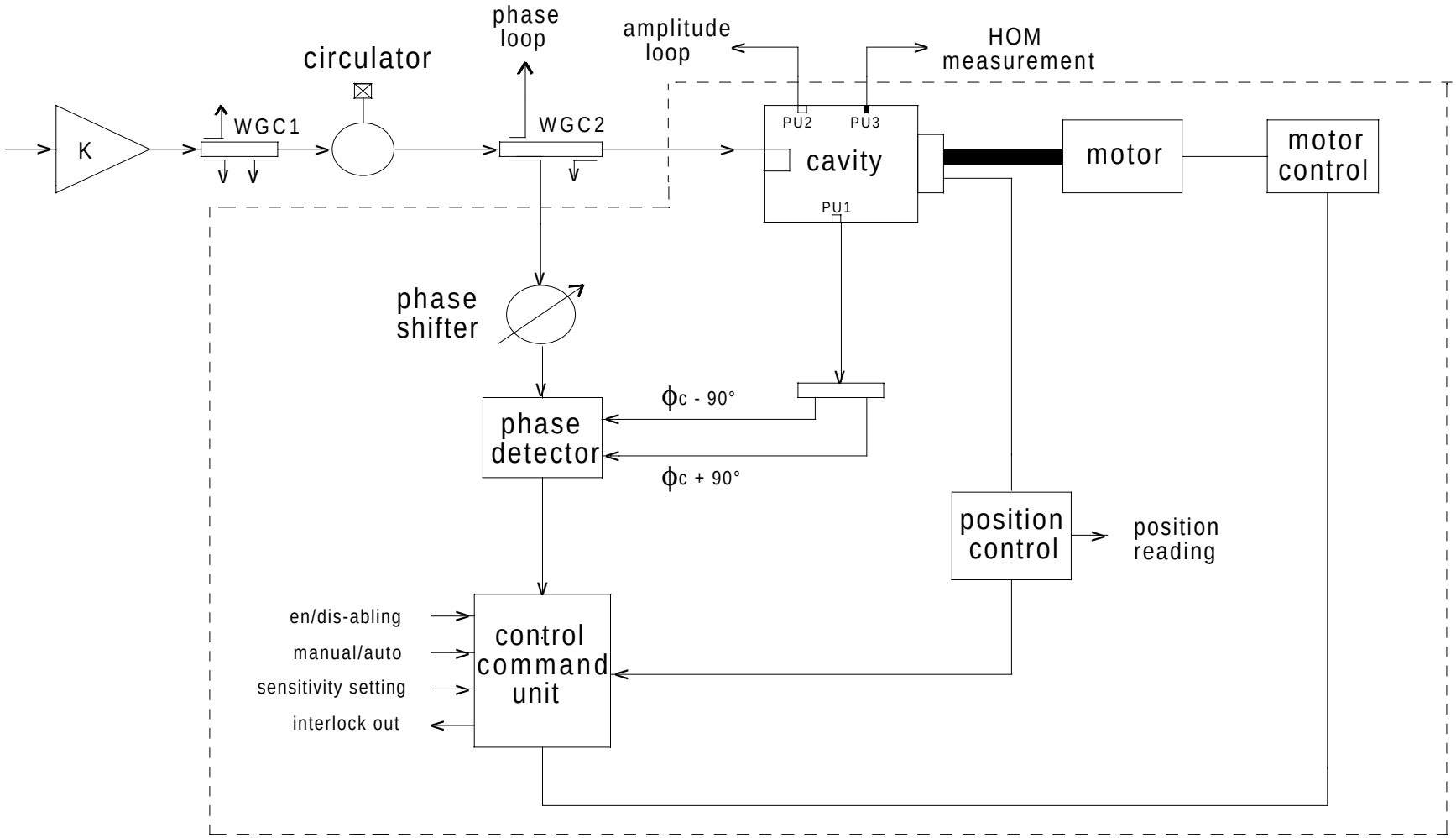

Figure f255_c : Block diagram of the frequency tuning loop.

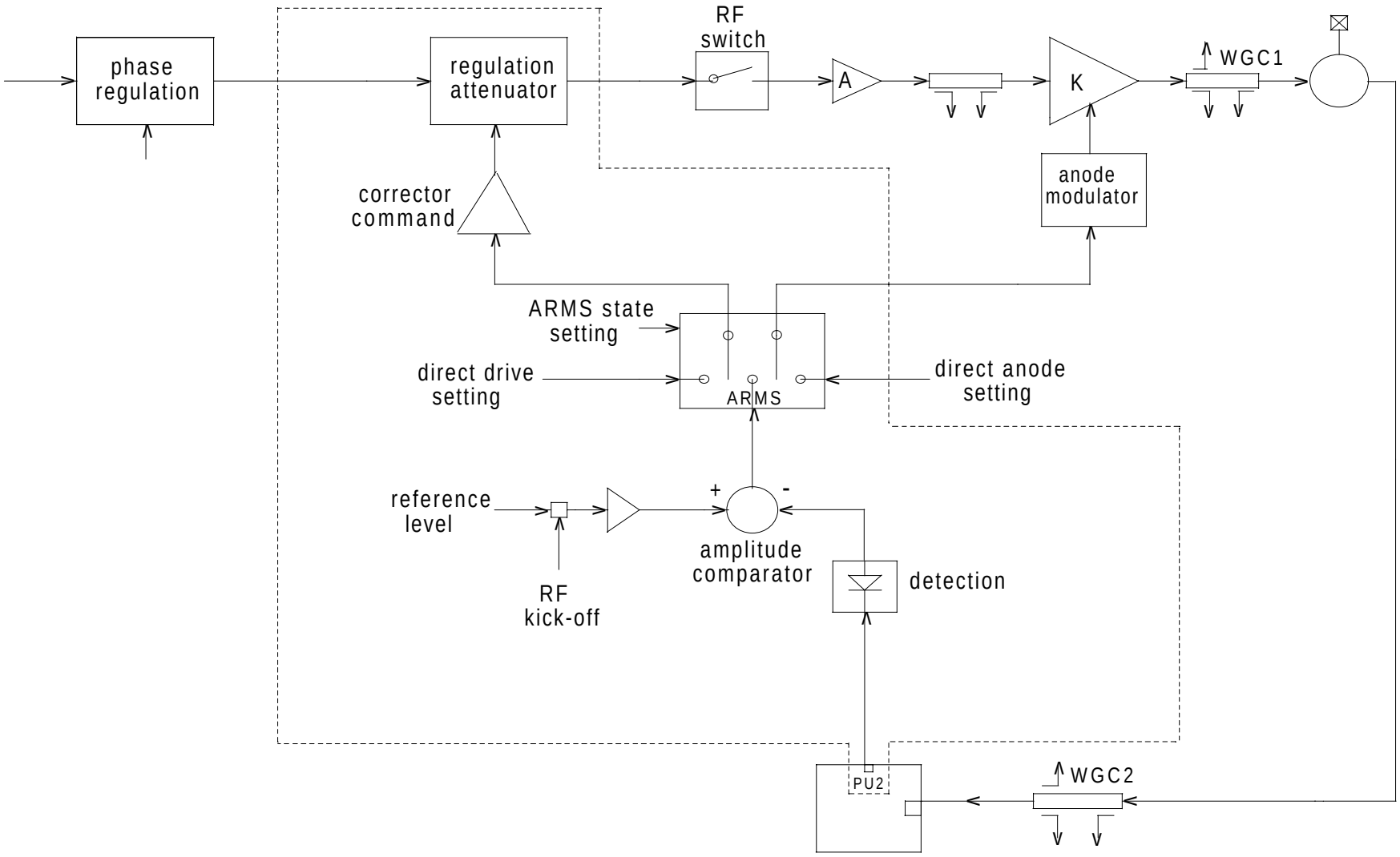

Figure f255_d : Block diagram of the amplitude loop (ARMS: Amplitude Regulation Mode Switch).

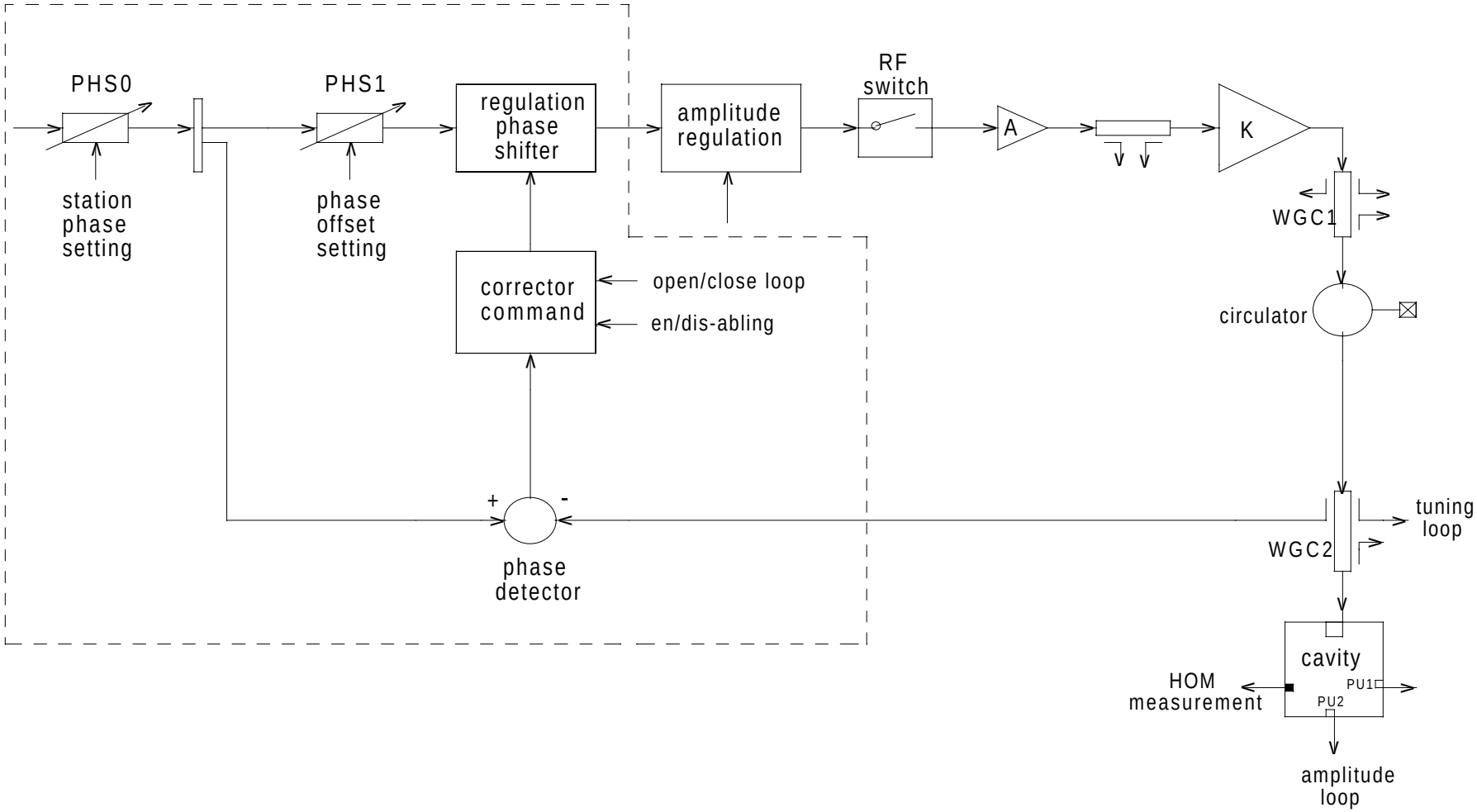

Figure f255_e : Block diagram of the phase loop.

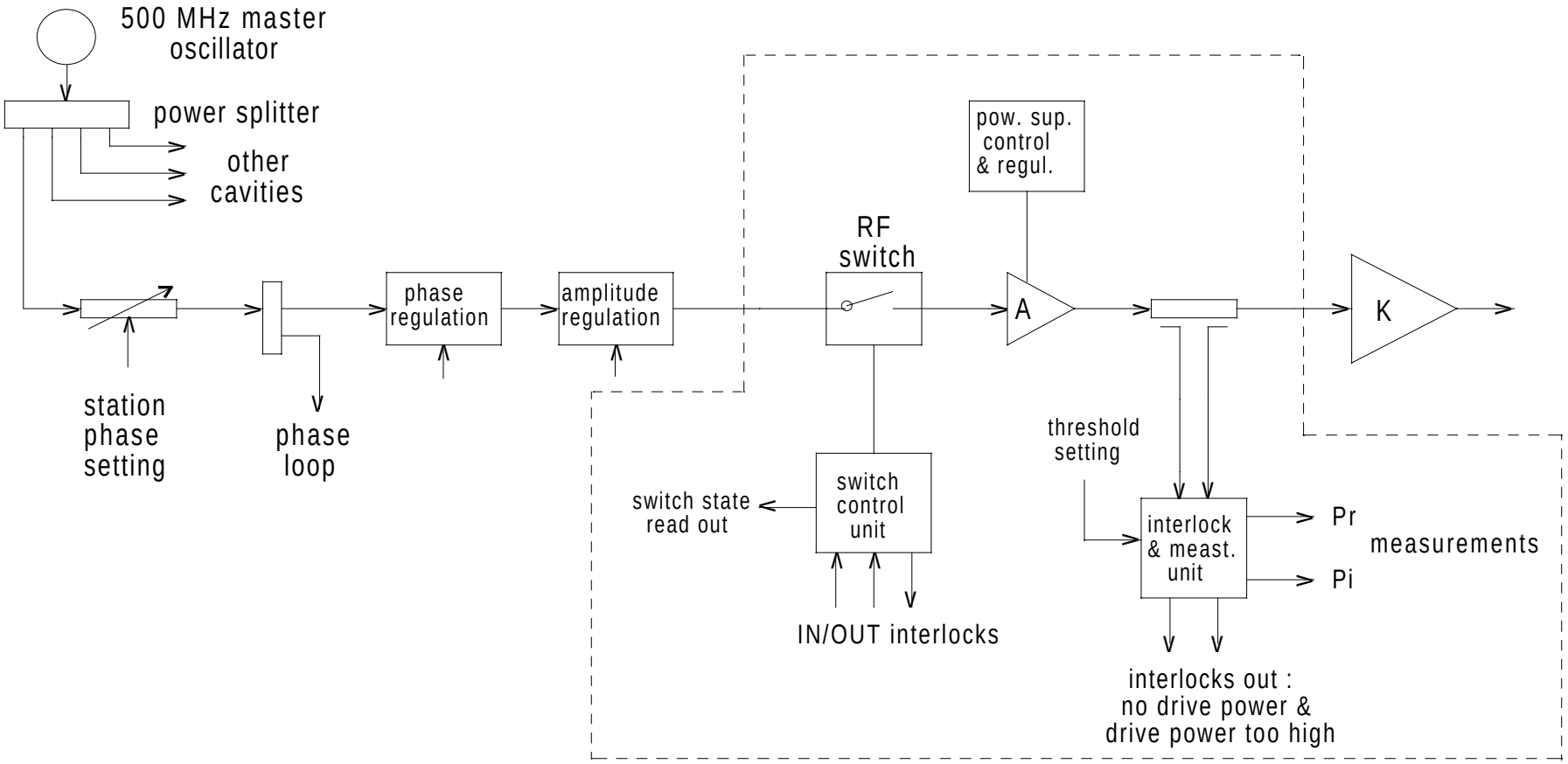

Figure f255-f : Block diagram of the drive chain.

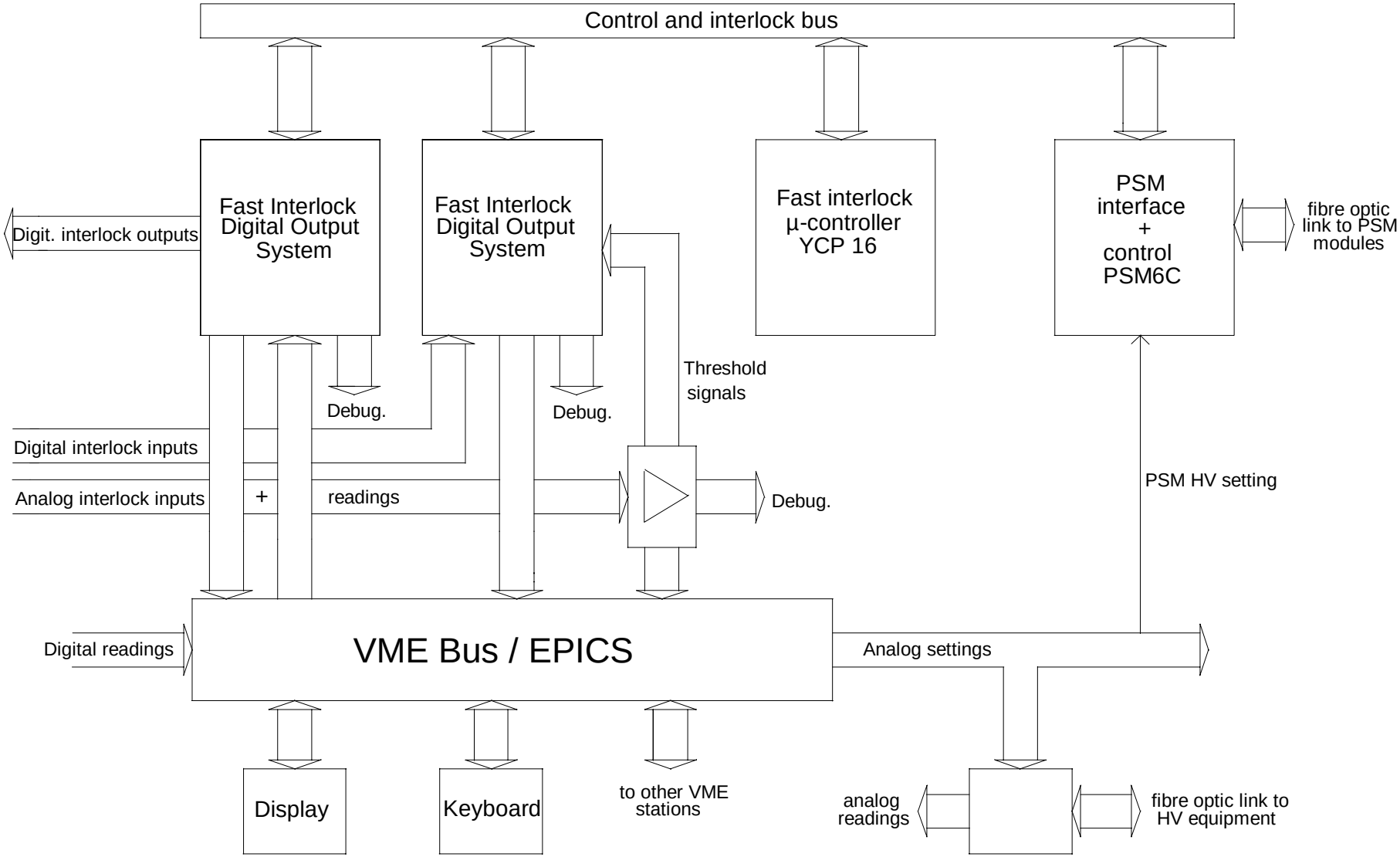

Figure f256_a : Block diagram of the RF control

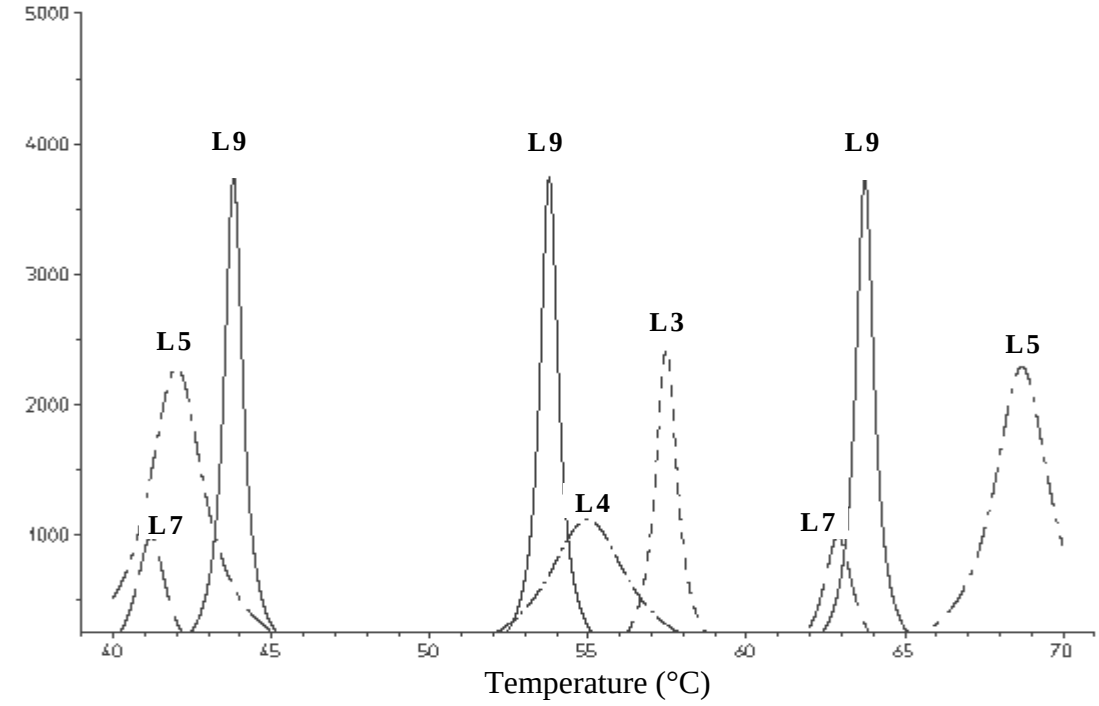

Figure f257_a: Growth rates of the longitudinal CBI versus cavity temperature (HOM parameters from Table t257_a).

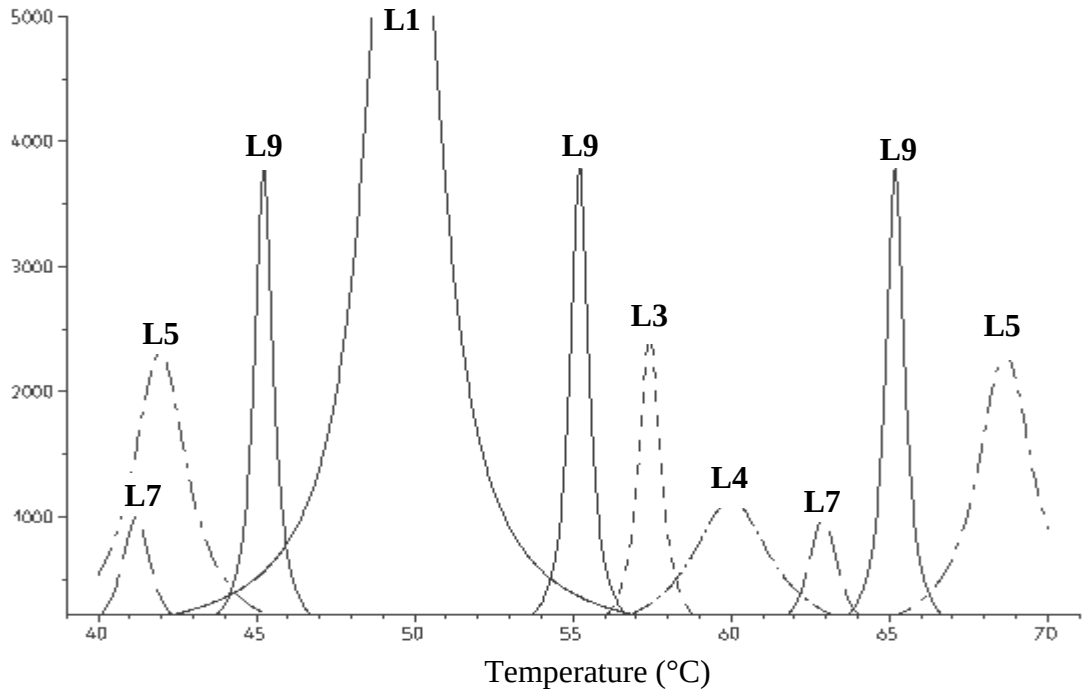

Figure f257_b: As above, but the HOM frequencies have been artificially set such that to simulate the most unfavourable case.

Figure f258_a : Phasor representation of the beam induced voltage in an idle cavity.

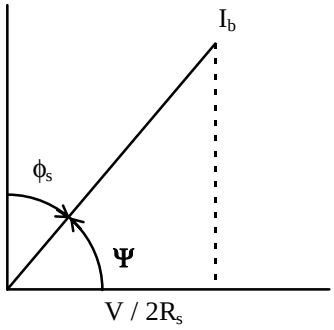

$V = 2\ R_s\ I_b \cos\psi = I_b \sin\psi\ (R/Q)\ f_r / \delta f;$
$P = V\ I_b \cos\psi = - V\ I_b \sin\phi_s = V^2 / (2\ R_s);$
$\phi_s = \psi - \pi / 2;$
ϕ_s is the synchronous phase;
ψ is the cavity tuning angle defined as:
$tg\ \psi = 2\ Q\ \delta f / f_r$.

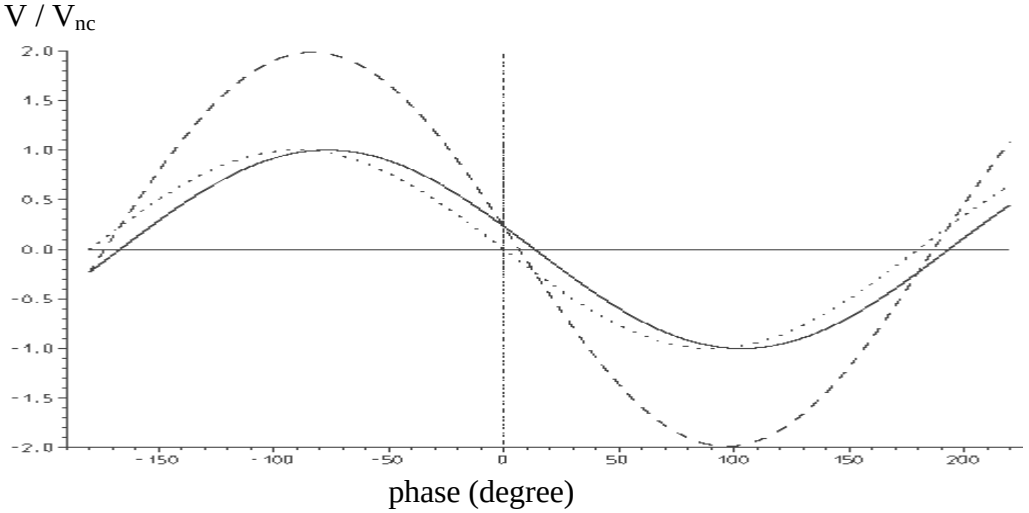

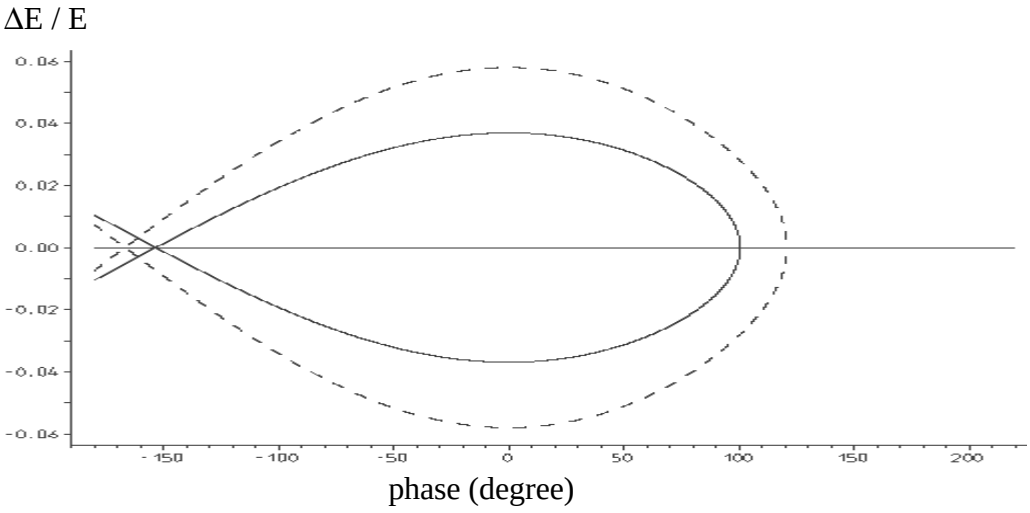

Figure f258_b : Normalised voltages (nc, sc, nc+sc) versus phase and "RF buckets" (nc and nc+sc) for $V_{nc} = V_{sc} = 2.6$ MV and $f_{nc} = f_{sc} = 500$ MHz.

V / V_{nc}

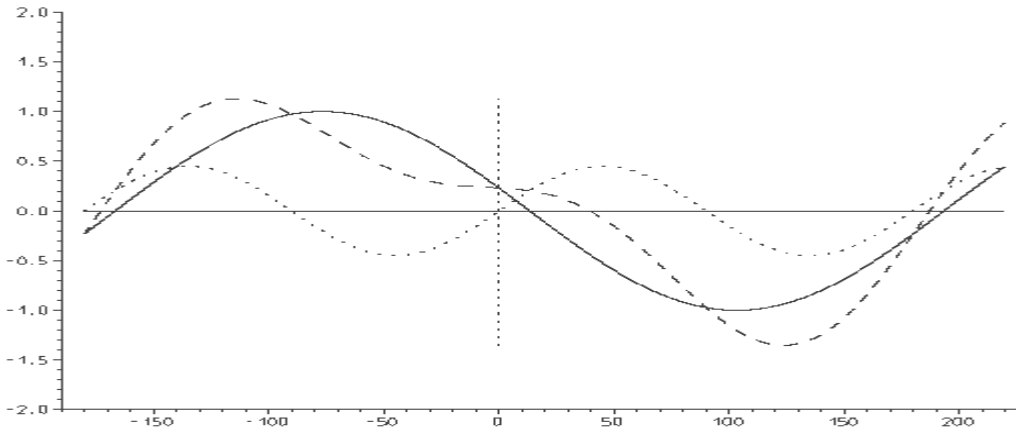

phase (degree)

$\Delta E / E$

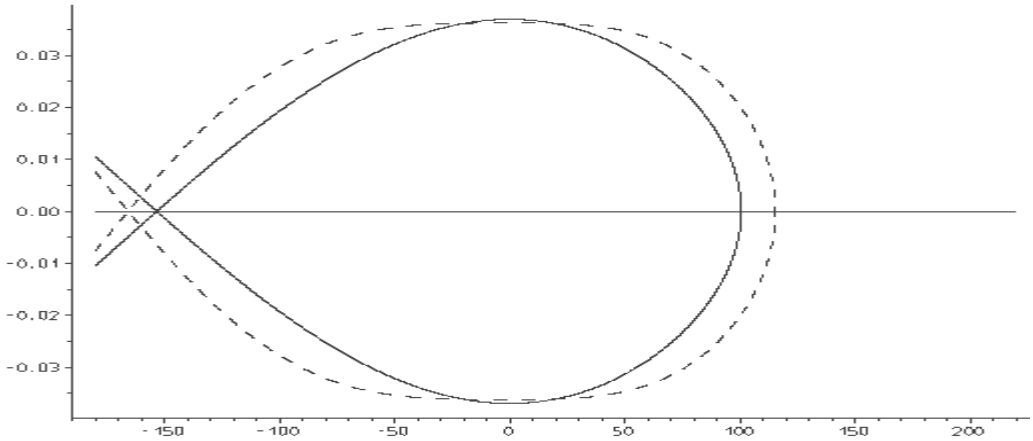

phase (degree)

I / I_o

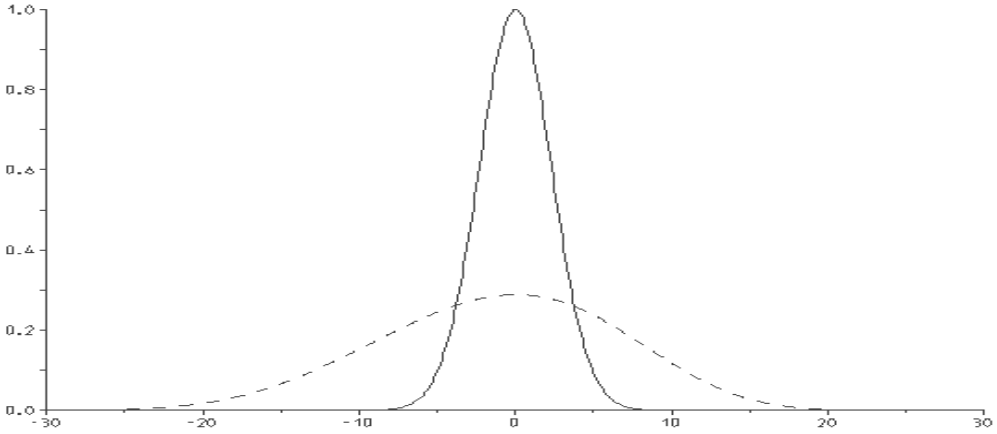

phase (degree)

Figure f258_c : Normalised RF voltages (nc, sc, nc+sc) versus phase, "RF buckets" and bunch profiles (nc, nc+sc) for V_{nc} = 2.6 MV, V_{sc} = 1.2 MV and $f_{sc} = 2.f_{nc}$ = 1 GHz.

V / V_{nc}

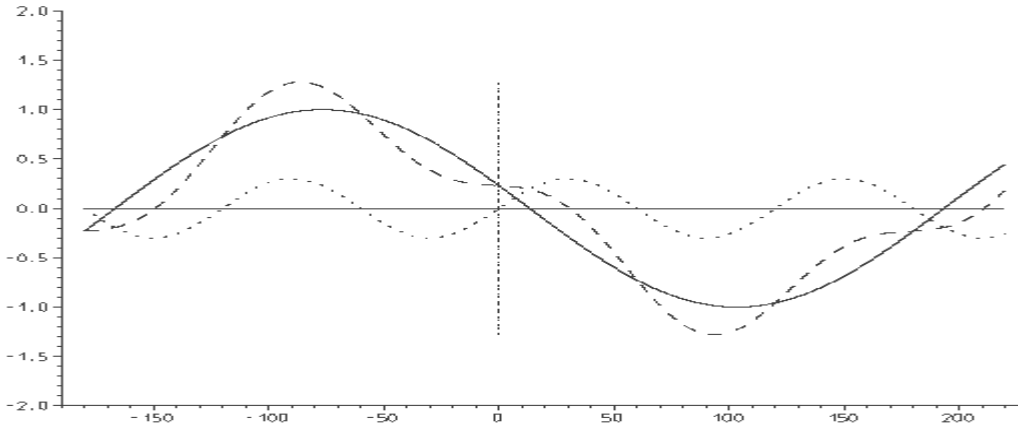

phase (degree)

ΔE / E

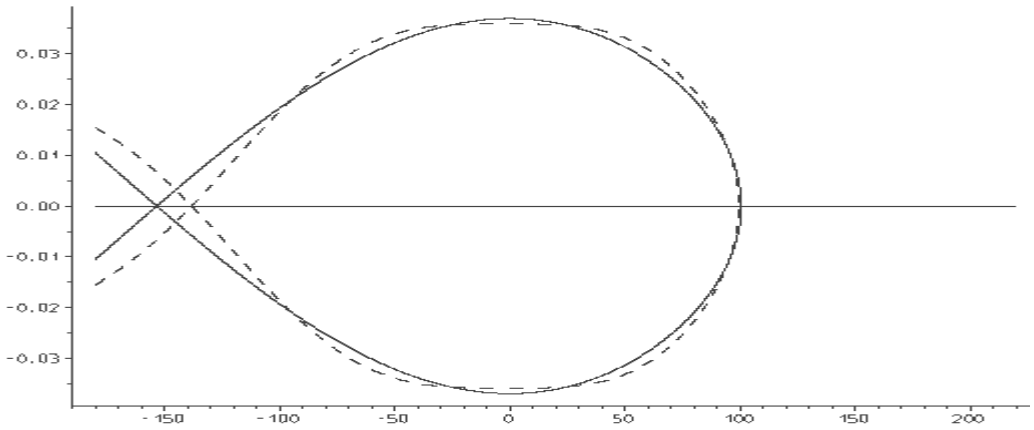

phase (degree)

I / I_o

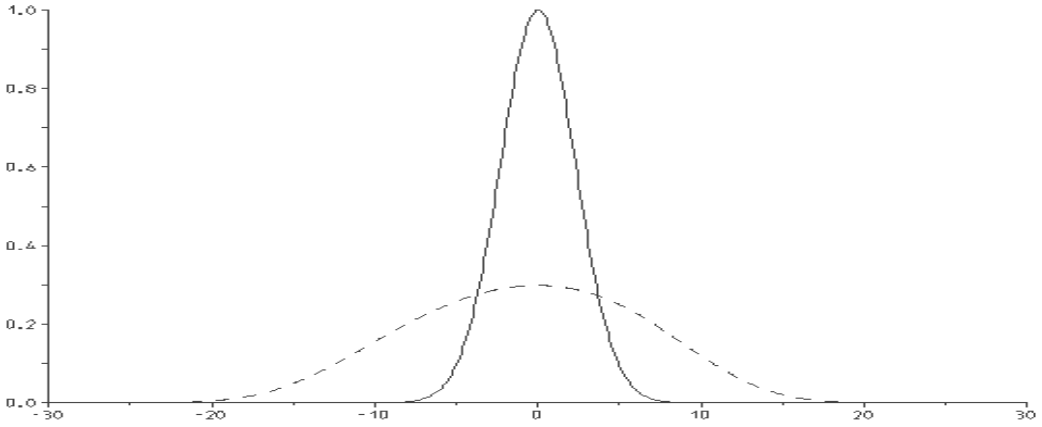

phase (degree)

Figure f258_d : Normalised RF voltages (nc, sc, nc+sc) versus phase, "RF buckets" and bunch profiles (nc, nc+sc) for V_{nc} = 2.6 MV, V_{sc} = 0.8 MV and $f_{sc} = 3.f_{nc}$ = 1.5 GHz.

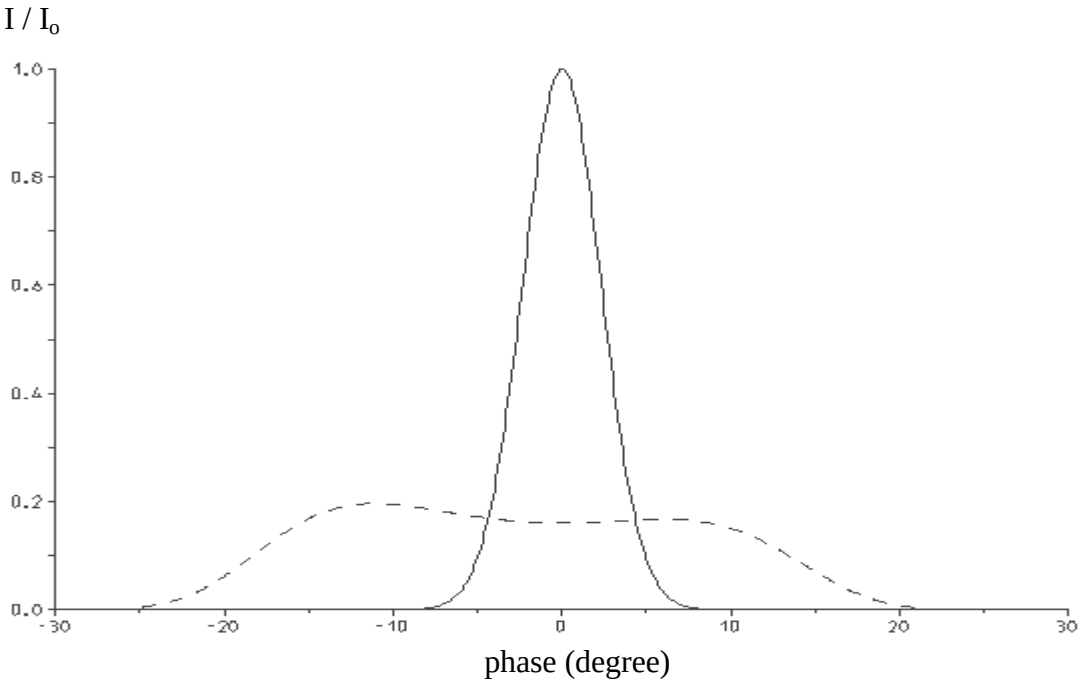

Figure f258_e : Distortion of the bunch profiles due to strong non linearity of the RF voltage ($V_{nc} = k*V_{sc}$).